Synthesis of Manganese Dioxide Nanoparticles Using *Andrachne Aspera* Root Extract for Antibacterial Activities

Betelihem Debebe Belete

A Thesis Submitted to the Department of Applied Chemistry,
College of Applied Natural Science
Presented in Partial Fulfillment of the Requirement for the Degree of Master's in Applied Chemistry (in Industrial chemistry)

Office of Graduate Studies
Adama Science and Technology University

February, 2026
Adama, Ethiopia

Synthesis of Manganese Dioxide Nanoparticles Using *Andrachne Aspera* Root Extract for Antibacterial Activities

Betelihem Debebe Belete

Advisor: Worku Dinku (Ph.D)

A Thesis Submitted to the Department of Applied Chemistry,
College of Applied Natural Science
Presented in Partial Fulfillment of the Requirement for the Degree of Master's in Applied Chemistry (in Industrial chemistry)

Office of Graduate Studies
Adama Science and Technology University

February, 2026
Adama, Ethiopia

Declaration

I hereby declare that this Master's Thesis entitled “Synthesis of Manganese Dioxide Nanoparticles Using *Andrachne Aspera* Root Extract for Antibacterial Activities” is my own work. That is not submitted for the award of any academic degree, diploma, or certificate in any other university and has not been submitted to any university. All sources of materials that are used for this thesis have been duly recognized by proper citations.

Betelihem Debebe	_____	_____
Name of student	Signature	Date

Recommendation

I, as the advisor of this thesis, hereby confirm that I have reviewed the revised version of the thesis titled “Synthesis of Manganese Dioxide Nanoparticles Using Andrachne Aspera Root Extract for Antibacterial Activities,” which was prepared under my supervision by Betelihem Debebe Belete. This thesis is submitted in partial fulfillment of the requirements for the Master of Science degree in Applied Chemistry (Specialization in Industrial Chemistry). Therefore, I endorse the submission of this revised thesis to the department in accordance with the relevant procedures.

Dr. Worku Dinku		
Advisor	Signature	Date

Approval Page

I am the advisor of the thesis entitled "Synthesis of Manganese Dioxide Nanoparticles Using *Andrachne Aspera* Root Extract for Antibacterial Activities." And developed by Betelihem Debebe Belete, hereby certify that the recommendations and suggestions made by the board of examiners are appropriately incorporated into the final version of the thesis.

Dr. Worku Dinku  _____

Major Advisor Signature Date

We, the undersigned, members of the Board of Reviewers of the proposal open defense by Betelihem Debebe Belete, have read and evaluated the thesis entitled "Synthesis of Manganese Dioxide Nanoparticles Using *Andrachne Aspera* Root Extract for Antibacterial Activities" and examined the candidate during the open defense. This is, therefore, to certify that the thesis is accepted for partial fulfillment of the requirements of the degree of Master of Science in Applied Chemistry (Industrial Chemistry)

_____ _____ _____

Chairperson Signature Date

_____ _____ _____

Internal Examiner Signature Date

Dr. Ali Mohammed  _____

External Examiner Signature Date

Final approval and acceptance of the thesis are contingent upon submission of its final copy to the Office of Postgraduate Studies (OPGS) through the Department Graduate Council (DGC) and School Graduate Committee (SGC).

_____ _____ _____

Department Head Signature Date

_____ _____ _____

College Dean Signature Date

_____ _____ _____

Office of Postgraduate Studies, Dean Signature Date

ACKNOWLEDGEMENT

First and foremost, I adore and honor Almighty God, the source of all wisdom, understanding, and insight!! I'd want to thank God for giving me the life and wisdom needed to complete my thesis. Next, I'd want to thank my adviser, Dr. Worku Dinku, for his invaluable counsel, insightful discussions, unwavering support, and direction. My heartfelt gratitude and honor also extend to my father, mother, and husband for their financial and emotional support. Thank you to all of my friends who have helped make my life meaningful and pleasurable. The memories of our relationship will live on in my heart. I will always be grateful to you, and may the Almighty reward you generously in fulfillment of my debt. Finally, I'd like to thank Adama Science and Technology University's Department of Applied Chemistry for their diverse support and kind assistance.

TABLE OF CONTENTS

CONTENTS **PAGE**

LIST OF FIGURES

LIST OF TABLES

LIST OF ABBREVIATION

NPs	Nanoparticles
MNPs	Metal Oxide Nanoparticles
MnO_2 NPs	Manganese dioxide Nanoparticles
UV-Vis	Ultraviolet-Visible Spectroscopy
XRD	X-ray Diffraction
FWHM	Full Width Half Maximum
FTIR	Fourier-Transform Infrared Spectroscopy
TGA	Thermogravimetric Analysis
DTA	Differential Thermal Analysis
VOCS	Volatile Organic Compounds
CVD	Chemical Vapor Deposition
ROS	Reactive Oxygen Species
MIC	Minimum Inhibitory Concentration
MHA	Muller Hinton Agar plate
MRI	Magnetic Resonance Imaging

Abstract

This study presents a bio-fabrication technique for MnO_2 nanoparticles utilizing Andrachne aspera root extract as a natural bio- agent. The phytochemicals inherent in the Andrachne extract perform a vital function in the bio-reduction of manganese ions and the steadying of the resultant tiny particles. The synthesized MnO_2 nanoparticles were systematically distinguished through ultraviolet-visible (UV-Vis) spectroscopy, Fourier-transform infrared spectroscopy (FTIR), X-ray diffraction (XRD), and thermal analysis (TGA/DTA). UV-Vis confirmed the formation of MnO_2 nanoparticles by exhibiting characteristic absorption features, with the measured band gap of the fabricated nanoparticles determined to range between 2.6 for 2.1eV, and 2.8 and 1.2 eV. FTIR analysis indicated the functional groups from the Andrachne extract in nanoparticle capping and stabilization. XRD analysis revealed that the MnO_2 nanoparticles possess a cubic face-centered phase structure, with crystallite sizes measured at 28.58 nm, 28.83 nm, and 25.83 nm corresponding to those synthesized with metal-to-bioextract ratios of 1:1, 2:1, and 1:2, respectively, and also the PH and concentration effect. The antibacterial efficacy of the produced MnO_2 nanoparticles was assessed against Gram-positive (Staphylococcus aureus) and Gram-negative (Escherichia coli) bacteria using the disc diffusion technique. The 2:1 MnO_2 sample synthesized using Andrachnes aspera root extract shows better antibacterial activity because this ratio optimizes the balance between phytochemical capping agents and MnO_2 nanoparticles. This leads to a smaller particle size, higher surface area, and stronger interaction with bacterial cell walls, enhancing oxidative stress and membrane disruption compared to other ratios. The nanoparticles demonstrated significant antibacterial activity, with inhibition zones increasing at higher nanoparticle concentrations. This is potentially due to a greater quantity of metallic precursors, potentially resulting in smaller and more reactive particles. These discoveries emphasize the capacity of biosynthesized MnO_2 nanoparticles as efficient antimicrobial agents. Overall, this study establishes a green, low-cost, and scalable synthesis route for producing bio-functional nanomaterials, with promising applications in biomedicine and environmental science.

Keywords: MnO_2 nanoparticles, green synthesis, Andrachne aspera extract, antibacterial activity

CHAPTER ONE

1. INTRODUCTION

1.1 Background of the Study

Metal nanoparticles (NPs) have distinct physicochemical features owing to their high surface area-to-volume ratio and nanoscale impacts (Muthukrishnan et al., 2025). Among them, manganese oxide nanoparticles (MnO_2 NPs) have received notice because of their numerous uses in disciplines including chemical sensors, ion sieves, rechargeable batteries, electrolysis systems, and microelectronics (Ahmed et al., 2025). Moreover, manganese-based nanomaterials are particularly appealing because Mn is an abundant and naturally occurring element. It is the 12^{th} naturally prevalent element in the Earth's crust and the 3^{rd} most abundant transitional metal after iron (Fe) and titanium (Ti). This renders Mangenese-based nanoparticles economically viable and suitable for industrial-scale application. In addition, MnO_2 NPs demonstrate excellent photocatalytic properties, especially in the removal of synthetic dyes under light irradiation (Karthik et al., 2025). Many approaches to nanotechnology synthesis are widely employed, including simple solution-based procedures, reactive precipitation, sol-gel, hydrothermal/thermal solid-state fabrication, electrochemical, and light-mediated reduction methods. Although physical and chemical technologies are available for the creation of tiny particles, green manufacturing is preferable due to its environmental friendliness and easy accessibility. The manufacture of nanoscales using plant extracts may be preferable to other biological techniques, such as the microbial route, which includes the time-consuming process of maintaining cell cultures (Malik et al., 2023).

The antioxidant properties of the plant extract are trustworthy for the fabrication of metal and metal oxide NPs (MONPs). antioxidant capacity assay, which is very notable for the fabrication of NPs. As noticed beyond, the production of NPs using plant extracts is known as a bio-fabrication technique (Martínez-cabanas et al., 2021). Manganese dioxide exists in several polymorphic crystal structures, including α- MnO_2 (hollandite), β- MnO_2 (pyrolusite), γ- MnO_2 (nsutite), δ- MnO_2 (birnessite), and κ-MnO_2 (akhtenskite). Although these phases share the same basic structural unit, MnO_6 octahedra, their properties differ due to variations in the way these octahedral units are interconnected. The distinct arrangement of MnO_6 octahedra results in different tunnel or layered structures, which significantly influence their physicochemical properties and suitability for various applications(Yang et al., 2023).

MnO_2 NPs can be created in either a top-down or bottom-up manner, and their structural linkages can be used to identify them. The top-down approach is not extensively employed due to its expensive preparation costs and structural faults in the produced NPs. The bottom-up approach is cheap to make and stable; they have been used in a variety of applications (Zhang et al., 2023). The tunnel-like a-MnO_2 was utilized as an electrolysis mediator for the elimination of oxygen and creation in both water and organic electrolytes (Salvador et al., 2021). Whereas stacked birnessite in particular is employed as a capacitor. Other MnO_2 polymorphs have likewise been utilized as adsorbents and catalysts in various applications (Hung et al., 2020). Synthesized MnO_2 NPs exhibit photo-catalytic performances for the dye degradation in the visible light region. The photo-catalytic properties for dye degradation of the synthesized MnO_2 NPs were investigated by the degradation of acid orange dye. Manganese oxide nanoparticles are widely utilized for dye removal owing to the strong chemical and physical interaction between their inorganic components (manganese dioxide nanoparticles) and organic (polymeric) matrices (Karthik et al., 2025). MnO_2 NPs are not simply harmless; they also have a highly active and powerful oxidation state. Since Mn has an oxidation number of +4. Additionally, manganese oxide particles have been utilized as an adsorbent, and catalytic investigation is focused on the capacity of Fenton catalyst-mediated oxidation of metal oxides, particularly manganese dioxide, to degrade dye molecules (H. Li et al., 2022).

The antibacterial performance of MnO_2 NPs fabricated via a green process has gained noteworthy interest, specifically in the face of rising antibiotic resistance. These nanoparticles have demonstrated efficacy against a multiplicity of Gram-positive and Gram-negative bacteria, such as Escherichia coli, Pseudomonas aeruginosa, and Staphylococcus aureus. The suggested procedures of antibacterial action include the generation of reactive oxygen species (ROS), damage to bacterial cell membranes, release of metal ions, and interruption of essential enzymatic processes. When synthesized using plant extracts like andrachne, the antibacterial effect may be amplified due to synergistic interactions between the bioactive compounds and the nanoparticles(Nguyen et al., 2023). In light of the above, this research concentrates on the photo-fabrication of MnO_2 NPs utilizing *Andrachne aspera* root isolate as a bio-agent. The produced NPs were distinguished by employing numerous analytical methods, such as ultraviolet-visible (UV-Vis), Fourier-transform infrared (FTIR), and X-ray diffraction (XRD), to determine their optical, chemical properties, and structural properties. Furthermore, their antibacterial activity was

evaluated against selected bacterial strains to assess their potential as antimicrobial agents. This research was expected to contribute to the development of sustainable, biocompatible nanomaterials with enhanced antibacterial properties, offering a viable alternative to chemically synthesized nanoparticles and supporting the global effort toward green and sustainable nanotechnology.

1.2 Statement of the Problem

The increased prevalence of bacterial diseases that cannot be effectively treated with antibiotics poses a serious global health challenge, which calls for an elevated level of research to design novel antimicrobial drugs. Conventional chemical approaches used for nanoparticle synthesis are responsible for health hazards and environmental pollution because of toxic reagents, solvents, and chemicals. Hence, the production of MnO_2 NPs using tree extract from Andrachne aspera would be a novel and recyclable method to address these challenges. The tannin-rich extract offered as a natural bio, agent, may also account for the better antibacterial activity of MnO_2 NPs. But its mechanism of interaction with bacteria is not significantly explored. Hence, the present work aims to address the same by investigating the biosynthesis of MnO_2 NPs using Andrachne aspera root extract and evaluating their anti-bacterial activity. This will influence the adoption of these natural antimicrobial roots for robust development of original discovery applications (Asfaw et al., 2023).

The formation of MnO_2 NPs using Andrachne aspera root extract bears huge scope for green and sustainable synthesis of nanomaterials. Exploiting the essence of phytochemicals present in the natural extract as mediators will propel forward the implementation of antimicrobial nanomaterials. To bring about the aforementioned benefits, it is imperative to fine-tune the synthesis parameters of MnO_2 NPs to achieve their many-fold improved efficiency due to various factors such as precursor-to-extract ratio, pH, precursor composition, and precursor concentration (Oliveira da Silva et al., 2024). Tuning the pH and precursor concentration optimizes the surface reactivity, growth directions, and shapes of MnO_2 NPs for antimicrobial effect. Achieving these parameters is therefore essential to ultimately engineer the antibacterial abilities of MnO_2 NPs, so that they can be considered for biomedical and environmental uses. This method would fulfill environmental chemistry objectives and stand as an economical route to the creation of functional nano-materials(Saod et al., 2022). The main challenge between non-biogenic synthesis methods

and this plant-based method is that the former involves high temperature, energy, and toxic chemicals, while the plant-based method is low-cost and biocompatible, but is impaired in its effective application due to difficulties in controlling particle size, distribution, and morphology.

1.3 Objectives of the Study

1.3.1 General Objective:

The principal purpose of this investigation was to prepare and characterize MnO_2 NPs synthesized utilizing Andrachne aspera root extract and evaluate their antibacterial properties.

1.3.2 Specific Objectives:

- To collect and extract the root of Andrachne aspera using distilled water.
- To identify the major phytochemicals of the *Andrachne aspera* root.
- To synthesize MnO_2NPs by using the aqueous extract of the *Andrachne aspera* root.
- To characterize the produced MnO_2 NPs utilizing TGA/DTA, UV-Vis, XRD, and FTIR.
- To evaluate the antibacterial activity of plant crude extract and manufactured MnO_2 NPs versus Gram-positive and Gram-negative bacteria.

1.4 Significance of the Study

The significance of the investigation in the synthesis of MnO_2 NPs lies in promoting a sustainable cost effective and biocompatible method, while also contributing to advancement in nanotechnology and environmental applications. The synthesis of MnO_2 NPs using *Andraea aspera* root extract is significant because it provides an eco-friendly, low-cost, and biocompatible method for producing advanced materials that can benefit society through applications in medicine, environmental protection, and sustainable technology**.** This research will bring a technology transfer and also initiate researchers to explore the use of *Andraea aspera* root for the synthesis of nanoparticles. It is also hoped that it will be used as one possible means of plant-mediated biological synthesis of MnO_2 NPs of desired quality with low cost, eco-friendly, and suitable techniques of preparation, so that the toxicity or hazardous nature of the chemical processes of synthesizing MnO_2 NPs can be avoided.

1.5 Scope of the Study

The choice of the explore on the *Andrachne aspera* root for antibacterial activities elaborates the withdrawal and recognition of bioactive compounds from the plant's root and their subsequent evaluation for antimicrobial properties. This research focused on the capacity of *Andrachne aspera* as a biological source of antibacterial substances to reduce bacterial illnesses, specifically those instigated by drug-resistant strains. The study included the screening of the root extracts against a range of bacterial pathogens, followed by the estimation of the smallest inhibitory concentration (MIC) and the method of exploitation of the active compounds. Furthermore, the research explored the chemical composition of the extracts, identifying specific phytochemicals responsible for the antibacterial effects. This study aimed to add to the expansion of alternative, plant-based antibacterial therapies and to present a better recognition of the therapeutic capacity of *Andrachne aspera* in addressing emerging microbial resistance. In this work, the extraction of the *Andrachne aspera* root took place, and the extract was utilized to produce MnO_2 NPs. The created samples were distinguished utilizing a UV-Vis spectrophotometer, XRD analysis, FT-IR, and TGA

CHAPTER TWO

2. LITERATURE REVIEW

2.1 Nanoparticles

Nanoparticles are defined as matter that has at least one physical dimension within the 1- 100 nm size range, where new size-dependent physical, chemical, and biological activities emerge and vary significantly from those of bulk materials. In the nanoscale, the large surface area-to-volume ratio, along with quantum confinement and changed electronic bands, contributes substantially to the enhanced reactivity, optical, and biological responses. These rare features have been the main drivers behind extensive research and the turning of nanoparticles into a variety of sectors, such as biomedicine, environmental applications, energy storage and conversion, catalysis, and agriculture (Eker et al., 2024). Depending on their material composition, nanoparticles are metals, metal oxides, polymeric, carbon-based, and composite nanomaterials, among which MONPs, such as MnO, ZnO, CuO, TiO, and FeO, have attracted special popularity due to the reasons of thermal stability, easy electronic modification characteristics, and widespread uses (Altammar, 2023). Nanomaterials are highly influenced by biological and physicochemical parameters such as surface chemistry, degree of agglomeration, morphology, particle size, and crystallinity. As an increase in the proportion of surface atoms increases, a decline in particle size occurs, thus improving chemical reactivity and surface strength. This effect is particularly pronounced in the antimicrobial device, as small nanoparticles are better able to penetrate the contact with a microorganism's cell membrane and intercellular structures. In addition, functional groups and surface defects on the nanoparticles can promote the generation of reactive oxygen species (ROS) that cause oxidative stress among microbial cells and lead to their damage. These features highlight the importance of a good controlled nanoparticle processing to tailor nanoparticle properties for a specific application (Eker et al., 2024; Tadesse & Hailemariam, 2025). Nanoparticles are made using numerous methods, such as physical, chemical, and biological, each having its own benefits and drawbacks. The physical and chemical methods typically consume a lot of energy and/or involve the use of toxic chemicals, whereas the green or biological synthetic routes are preferred because of their eco-friendliness, low cost, and the use of renewable sources (Ula et al., 2025). In addition, the recent studies on the preparation of nanocomposites, which are formed by combining

two or more different nanomaterials, have been mainly focused on the resulting synergistic effect, improved stability, and functional performance.

2.2 Metal Oxide Nanoparticles

MO NPs are nanoscale materials made up of metal elements and oxygen, having different physical, chemical, and biological attributes that differentiate them from their bulk counterparts. These nanoparticles' substantial surface area, reactive nature, and ability to undergo numerous surface changes make them exceedingly flexible in numerous types of applications. Common examples of MONPs include titanium dioxide (TiO_2), zinc oxide (ZnO), copper oxide (CuO), manganese dioxide (MnO_2), and iron oxide (Fe_2O_3, Fe_3O_4). Due to their exceptional properties, metal oxides are widely utilized in fields such as catalysis, energy storage, environmental remediation, and biomedical applications. For instance, they are used as catalysts in chemical reactions, as electrodes in batteries and supercapacitors, and as antimicrobial agents in medical and environmental settings. Their capacity to cooperate with light, chemicals, and biological systems allows for innovative applications, though concerns about their toxicity and environmental impact continue to drive research into safer and more sustainable synthesis methods(Aigbe & Osibote, 2024; Radulescu et al., 2023).

Bio-fabrication of MnO_2 NPs utilizing medicinal plant extracts has shown promising antibacterial properties, offering a low-cost, eco-friendly alternative to conventional routes and enabling bioactive surfaces that disrupt pathogens. For instance, MnO_2 NPs biosynthesized with Datura stramonium leaf extract exhibited clear formation verified by UV–Vis spectroscopy and demonstrated antimicrobial efficacy, highlighting the practicality of phytochemical-driven reduction and capping for stability and bioactivity (Pole et al., 2025). Beyond particulate forms, MnO_2 nanosheets display potent bactericidal effects via reactive oxygen species (ROS) generation and membrane integrity destruction, underscoring oxidative stress and envelope damage as key mechanisms of action against both Gram-positive and Gram-negative strains (Du et al., 2020). Microbial routes also confirm broad feasibility: Bacillus subtilis cell-free supernatant can reduce manganese salts to MnO_2 NPs with measurable antibacterial effects, suggesting that biomolecules (enzymes, proteins, metabolites) drive nucleation and functionalization that enhance interaction with bacterial membranes (Ogunyemi et al., 2020). Framing Andrachne aspera root extract within this literature, its phenolics, alkaloids, and reducing sugars are likely to act as dual reducing and

stabilizing agents, yielding MnO2 NPs capable of ROS-mediated killing and membrane disruption similar to plant- and microbe-derived counterparts; comparative evaluation should therefore profile size, crystallinity, zeta potential, and phytochemical capping via UV–Vis, FTIR, XRD and assess antibacterial activity against model organisms (e.g., S. aureus, E. coli) through zone of inhibition, MIC, and ROS assesses to benchmark against prior Datura-based particles and nanosheets mechanisms (Ghosh et al., 2022).

2.3 Manganese Oxide Nanoparticles

Manganese oxide is one of the most intriguing materials, incorporating a wide range of structures with a huge surface area. The varied structures and chemical properties of manganese oxides are taken advantage of for potential application like as ion and molecule separation, battery, cation-exchange, sensor absorbents, catalysis, etc. MnO_2 comes in four valence states: MnO (Mn^{+2}), Mn_3O_4 ($Mn^{+2.67}$), Mn2O3 (Mn^{+3}), and MnO_2 (Mn^{+4}). The valence state indicates the field of applicability. MnO2 is utilized as an electroactive material in lithium-ion battery systems and as a catalyst in oxidation-reduction reactions. The existence of Mn^{+3} ions in the MnO_2 lattice, known as MnO-OH, causes electron transfer between Mn^{+4} and Mn^{+3} ions. This process is what gives non-stoichiometric manganese oxide its catalytic activity (Mokaba et al., 2024).

Mn_2O_3 has proven useful in the production of soft magnetic substances, and it also catalyzes the removal of carbon monoxide from waste gas. Mn_3O_4 ($Mn^{+2.67}$) has attractive electronic properties, such as the change of its transmittance in the visible spectrum with an applied voltage, making it a candidate for window applications. Several processes were used to deposit manganese oxide thin films, including atomic layer deposition, liquid-phase electrochemical method, pulsed laser deposition, chemical bath deposition, electron beam deposition, thermal evaporation, hydrothermal, sol–gel, and chemical spray pyrolysis (Horti et al., 2024). They have a modest band gap but a high optical constant. Co-chemical approach development is being made; for example, this method allows for simple, easy management of the size and composition. There are several requirements for converting the particle surface state and achieving complete identity. The easy chemical process of various salts (Manganese nitrates, Manganese sulphate, and Manganese chlorides) with an excellent control of pH by utilizing NaOH solutions results in appropriate spinel oxide nanoparticles (Hessien et al., 2025).

2.4 Manganese Dioxide (MnO_2) Nanoparticles

Manganese dioxide nanoparticles have gained substantial attention owing to their various crystal structures, outstanding catalytic performance, and multifunctional applications. They are extensively employed in environmental remediation, energy storage devices, chemical sensors, and biomedical technologies. Their remarkable redox behavior and chemical stability make them promising materials for supercapacitors and battery systems. In addition, their biocompatibility and ability to generate reactive oxygen species (ROS) have expanded their potential in biomedical fields, including antimicrobial applications, cancer therapy, and drug delivery (Velho Pereira et al., 2026). MnO_2 NPs can be fabricated through various techniques, including sol–gel, hydrothermal, electrochemical, sonoelectrochemical, and green synthesis using plant extracts. Green synthesis methods are particularly advantageous because they are sustainable, affordable, and reduce reliance on toxic reagents. These controlled and solvent-free or template-free techniques enable the production of tailored nanomaterials for advanced technological and environmental applications (Jiang et al., 2024). Structurally, MnO_2 exhibits multiple polymorphic forms built from interconnected MnO_6 octahedra. It consists of planar O–Mn–O zigzag chains arranged in the *ac* crystallographic plane, and its structure is strongly influenced by the coupling geometry of these chains. At ambient temperature, MnO_2 has a band gap energy around 2.19 eV and displays n-type semiconductor behavior, where electrons serve as the primary charge carriers. These electronic properties make it suitable for photocatalytic and electrochemical applications. Transition-metal oxides such as MnO_2 are ideal electrode materials due to their chemical stability and variable valence states, leading to applications in alkaline batteries, electrochemical capacitors, smart windows, gas sensors, and photocatalysts (Malhotra et al., 2024).

MnO_2 nanoparticles also exhibit significant antibacterial activity. Their antimicrobial effectiveness is closely related to their structural, optical, and thermal characteristics, as confirmed by UV–Vis spectroscopy, X-ray diffraction (XRD), and thermogravimetric analysis (TGA). Under UV irradiation, MnO_2 generates ROS, which spoil microbial cell membranes and DNA, ultimately causing cell death. UV–Vis analysis verifies their optical absorption in the UV region, indicating strong photocatalytic potential. XRD provides information about crystalline phase and particle size, where smaller crystallites offer larger surface areas for bacterial interaction and enhanced ROS production. TGA confirms their thermal stability, ensuring sustained structural integrity and prolonged antibacterial activity under varying environmental conditions (Fitriannisa et al., 2025).

Overall, the antibacterial performance of MnO_2 nanoparticles is not solely attributed to their chemical reactivity but is strongly dependent on their optical properties, crystallinity, and thermal stability. These combined features make MnO_2 a highly promising material for environmental, energy, and biomedical applications

2.5 Synthesis Methods of Manganese Dioxide Nanoparticles

Manganese dioxide NPs can be manufactured utilizing a diversity of processes, each with unique advantages in terms of size, shape, and characteristics. Sol-gel extraction, hydrothermal co-precipitation, and reduction by chemicals are all common synthesis procedures. The sol-gel technique involves the transition of metal salts into a gel state, followed by heat treatment to form MnO_2 nanoparticles with controlled morphology and crystallinity. Co-precipitation is the simultaneous precipitation of manganese salts from a mixture under controlled conditions, yielding MnO_2 NPs. Chemical reduction methods utilize reducing agents to reduce manganese salts to MnO_2 in solution, allowing for the formation of tiny particles (Plakia & Kartsonakis, 2025). The hydrothermal method, which employs high temperature and pressure in a sealed environment, is often used to produce high-purity nanoparticles with uniform size (Lu et al., 2023). Bio-synthesis, which uses plant extracts or microbes, is gaining attention because of its sustainable nature and ability to produce biocompatible MnO_2 nanoparticles with enhanced properties. Each of these methods allows for tailoring the size, shape, and crystalline structure of the NPs, so this property is crucial for their performance in uses such as catalysis, pollution control, and energy storage systems (Karthik et al., 2024).

2.5.1 Physical Synthesis Methods of MnO_2 NPs

Physical manufacturing methods for MnO_2 NPs primarily involve techniques that utilize physical energy sources to induce the formation of nanoparticles. One of the most common physical methods is the laser ablation method, where a high-powered laser is used to ablate a manganese target in a liquid medium, resulting in the formation of MnO_2 NPs. This approach provides for perfect control of particle size and shape, with the added advantage of being a solvent-free process (Corrales et al., 2022). Ball milling is another physical method in which manganese powder is subjected to mechanical grinding in a ball mill, causing the material to break down into fine particles, including MnO_2 nanoparticles. This method is relatively simple but may require

additional post-treatment to improve nanoparticle size uniformity (Mohite et al., 2025). Chemical vapor deposition (CVD) can also be employed to synthesize MnO_2 NPs by reacting manganese-containing gases in a high-temperature chamber, where MnO_2 nanoparticles form on a substrate surface. These physical techniques provide accurate regulation of particle size and crystalline structure, which directly affect their efficiency in catalysis, sensors, and energy storage systems (Hung et al., 2020).

Physical synthesis of MnO_2 NPs is limited by high energy demands, poor drawback over particle size and morphology, and scalability challenges. Physical methods such as ball milling, laser ablation, and sputtering are often employed to produce MnO_2 NPs, but they come with several drawbacks. These techniques generally require expensive equipment and significant energy input**,** making them less cost-effective compared to chemical or biological synthesis routes. Moreover, physical synthesis often struggles with controlling particle size distribution, surface area, and crystallinity**,** which are critical for uses in catalysis, energy storage, and biomedical fields. The subsequent nanoparticles may show non-uniform shapes and agglomeration**,** reducing their functional efficiency. Another limitation is the low yield and poor scalability, as physical methods are not easily adaptable for large-scale industrial production. Additionally, the absence of stabilizing agents in purely physical processes can lead to instability and reduced biocompatibility**,** restricting their use in medical or environmental applications (Al-Harbi & Abd-Elrahman, 2025).

2.5.2 Chemical Synthesis of MnO_2 NPs

Chemical fabrication techniques are broadly utilized to create MnO_2 NPs due to their ability to offer control over particle size, morphology, and structure. One of the most common methods is co-precipitation, in which manganese salts, such as manganese chloride or manganese sulfate, are mixed with alkaline solutions (like sodium hydroxide or ammonium hydroxide) to precipitate MnO_2 in the form of nanoparticles. The concentration of reagents, pH, and temperature are carefully monitored to attain the desired particle size and crystal structure (Yadav & Bhaduri, 2023). Another widely used technique is hydrothermal synthesis, where manganese precursors are subjected to high-pressure and high-temperature conditions in a sealed vessel, promoting the formation of crystalline MnO_2 nanoparticles. This method often leads to high-purity and uniform nanoparticles with controlled morphology. Sol-gel synthesis is also frequently applied, where manganese salts are mixed with a gelling agent, followed by heat treatment to form MnO_2

nanoparticles. This approach enables fine control over the surface area and structure of nanoparticles. Furthermore, chemical reduction methods involve reducing manganese salts via reduction agents such as sodium borohydride or hydrazine to produce MnO_2 NPs. These methods are attractive due to their effortlessness and capacity to produce nanoparticles in solution. Chemical methods are highly versatile and can be adapted to produce MnO_2 NPs with tailored properties for various applications, including medical devices, ecosystem protection, energy storage, and catalysis (Gul et al., 2025).

In materials science and chemistry, a wide range of synthesis methods have been developed to tailor the structural, morphological, and functional characteristics of compounds. Among the most widely reported approaches are hydrothermal and solvothermal techniques, which include crystallization of materials from aqueous or non-aqueous solutions under high temperature and pressure conditions. These methods are particularly effective for producing nanostructures with controlled size, shape, and crystallinity(Kang et al., 2023). In contrast, precipitation and co-precipitation methods are simpler, solution-based techniques that rely on the formation of insoluble products through chemical reactions in liquid media. Precipitation is often used for bulk material preparation, while co-precipitation allows for the simultaneous incorporation of multiple ions, making it valuable for synthesizing mixed oxides, doped materials, or composite structures. Collectively, these methods are extensively discussed in the literature due to their versatility, scalability, and ability to influence the physicochemical characteristics of the final products, thereby enabling applications in catalysis, energy storage, environmental remediation, and biomedical fields (Z. Li et al., 2023).

2.5.3 Green Synthesis of MnO_2 NPs

Nano-sized particles can be made utilizing a variety of conventional processes. Natural synthesis pathways are more effective than physical and chemical methods. Bio-fabrication has arisen as an alternative to conventional approaches, overcoming their limitations. Phyto-fabrication is primarily concerned with the reduction of toxic substances and the exploitation of sustainable procedures, including the adoption of environmentally conscious ingredients, solvents, and recyclable materials. Different metal tiny particle manufacturing methods have been stated in green nanotechnology, including yeast, fungi, bacteria, algae, and plant extracts (Vanga & Satla, 2025). From an environmental standpoint, the use of plant extracts in the fabrication represents a

more green and biodegradable method to metal NP production associated with conventional chemical and microbial techniques. Plant-mediated creation offers significant advantages due to the rich diversity of bioactive complexes present in plant extracts. These phytochemicals, such as flavonoids, phenolics, alkaloids, and proteins, serve as natural bio-agents during NP formation. The presence of these biomolecules enhances the rate of metal ion reduction and improves the strength of the NPs. Furthermore, green synthesis using plant extracts can be carried out under mild and environmentally benign conditions, including relatively low reaction temperatures and atmospheric pressure, making the process simple, cost-effective, and sustainable (Hano & Abbasi, 2022). The flow chart in Figure 1 indicates the procedures of green synthesis.

Figure 1: Green synthesis of MnO2 NPs

Bio-fabrication of MnO_2 NPs is a recyclable and sustainable method that utilizes biological sources, including plant extracts, microbes, and natural polymers as bio-agents. This approach is gaining popularity because of its low environmental impact, simplicity, and cost-effectiveness. In plant-mediated synthesis, various plant extracts rich in polyphenols, flavonoids, and other bioactive compounds can reduce manganese salts to form MnO_2 nanoparticles. The extracts not only act as reducing agents but also help stabilize the tiny particles by foiling the cluster. For example, extracts from plants like Andrachne aspera and Cinnamomic have been shown to

successfully synthesize MnO_2 nanoparticles with controlled size and morphology (Shanshool et al., 2024). Similarly, microbes such as bacteria, algae, and fungi have been surveyed for biosynthesis, where they facilitate the reduction of manganese ions to MnO_2 through enzymatic activities. This method offers the use of yielding biocompatible NPs with unique activity that can be utilized in applications like catalysis, energy storage, and antimicrobial activities. Moreover, green synthesis eliminates the poisonous chemicals and unkind situations, making it a sustainable option to traditional chemical processes. The use of natural resources in the synthesis process also ensures that the MnO_2 nanoparticles are environmentally friendly, biodegradable, and potentially safer for biological applications(Eweis et al., 2024).

Table 1: Green Synthesis of MnO_2 Nanoparticles Using Plant Extracts for Antibacterial Applications.

Plant Used (Extract)	Method of Synthesis	Characterization Techniques	Antibacterial Activity	Target Microorganisms
Viola betonicifolia (leaf extract)	Plant extract mixed with Mn precursor under controlled heating	UV–Vis, FTIR, SEM, TEM, XRD	Strong antibacterial activity due to phytochemicals reducing Mn salts	*E. coli*, *S. aureus*, *P. aeruginosa*
Azadirachta indica (Neem leaves)	Aqueous leaf extract acts as a reducing and stabilizing agent	UV–Vis, XRD, SEM	Inhibition zones observed against Gram-positive and Gram-negative bacteria	*Staphylococcus aureus*, *Escherichia coli*
Moringa oleifera (leaf extract)	Green synthesis via boiling extract with Mn salt solution	FTIR, TEM, XRD	Moderate antibacterial activity; enhanced with higher NP concentration	*Klebsiella pneumoniae*, *Bacillus subtilis*

Ocimum sanctum (Tulsi leaves)	Extract prepared in ethanol, reacted with Mn precursor	UV–Vis, SEM, EDX	Effective antibacterial activity due to bioactive compounds	*E. coli*, *S. aureus*
Trigonella foenum-graecum (Fenugreek seeds)	Seed extract used as a reducing agent	XRD, SEM, FTIR	Exhibits antibacterial zones of inhibition	*Salmonella typhi*, *Staphylococcus aureus*
Camellia sinensis (Green tea leaves)	Polyphenol-rich extract reduces Mn salts	TEM, UV–Vis, FTIR	Strong antibacterial effect attributed to catechins	*E. coli*, *Pseudomonas aeruginosa*
Allium sativum (Garlic extract)	Garlic extract mixed with Mn precursor solution	SEM, FTIR, UV–Vis	Potent antibacterial activity due to sulfur compounds	*S. aureus*, *E. coli*
Zingiber officinale (Ginger root extract)	Ethanolic extract used for reduction	UV–Vis, XRD, SEM	Moderate antibacterial activity	*Bacillus subtilis*, *E. coli*
Lawsonia inermis (Henna leaves)	Henna extract reacts with Mn precursor	FTIR, SEM, TEM	Antibacterial activity observed; phytochemicals stabilize NPs	*S. aureus*, *Klebsiella pneumoniae*

2.6 Applications of MnO_2 NPs

Manganese dioxide (MnO_2) is a key semiconductor material that has been the focus of considerable research due to its technological and electrical characteristics. MnO_2 is a semiconductor oxide whose band gap is about 1.33 eV at room temperature. Owing to its excellent chemical and physical performance, MnO_2 has been used extensively in different fields. MnO_2 is one's first choice material for cathodes of secondary batteries. Besides that, its catalytic activity and ion exchange capacity turn it into a great material for biomedical applications, including magnetic resonance imaging (MRI). Since the functioning of MnO_2 in these purposes is highly reliant on the nanoscale size and crystal morphology of MnO_2, this has opened up a new field of research on MnO_2 nanoparticles. Moreover, MnO_2 not only has an excellent electrical conductivity similar to other functional materials, but it can exist in multiple oxidation states as well as various structural and chemical forms. Antimicrobial, antioxidant, and photocatalytic activities are among the most important uses of such a material (Suryawanshi et al., 2023).

Manganese's high catalytic activity, in combination with the considerable surface area of MnO_2 NPs as compared to their bulk forms, renders them great candidates for cleaning up contaminated soils. MnO_2 NPs have shown great efficacy in the removal of a variety of soil toxicants such as arsenic, selenium, thallium, cadmium, and lead. Additionally, MnO_2 has been effectively utilized to treat soil and water contaminated with industrial toxic dyes, as well as oestradiol, a hormone-disrupting compound that poses a risk to human beings and aquatic life (K.K. & Gangadharan, 2022). The electrochemical and oxidative traits of manganese oxides enable them to be particularly good candidates for the creation of nanocomposites that are reactive to a broad spectrum of chemical agents. With the help of MnO_2, biosensors have been fabricated for the detection of critical biological and chemical elements, such as β-glucosidase, glucose, and glutathione (GSH) in human blood, as well as pathogenic bacteria, Salmonella typhimurium, in food materials. Because of their exceptional physicochemical features, nanoparticles are becoming more popular for use in medicine. These discoveries have resulted in the rise of new fields such as nanomedicine and nano theranostics. Compared to traditional methods, nanomaterials present such substantial benefits as: better biocompatibility, increased cell targeting, and more efficient cellular internalization, which altogether unlock the potential for new biomedical applications (Chai et al., 2026).

2.6.1 Antimicrobial Application

2.6.1.1 Antibacterial Application

Manganese dioxide (MnO_2) has gained attention for its antibacterial properties, making it useful in various healthcare and environmental applications. It has been shown to exhibit antimicrobial activity by disrupting the cell walls of microorganisms and ROS, which can break bacterial cells and reduce their development. MnO_2 nanoparticles are particularly effective in fighting a wide-ranging band of microbes, including both Gram-positive and Gram-negative strains. These NPs can be integrated into coverings for medical uses, wound dressing, and water remediation systems to inhibit bacterial infections and reduce contamination. Furthermore, MnO_2's ability to decompose organic pollutants and pathogens in water has sparked its use in environmental cleanup processes. Its eco-friendly nature and relatively low toxicity make MnO_2 a promising material for developing sustainable antibacterial treatments and systems (Fitriannisa et al., 2025).

2.6.1.2 Antifungal Application

MnO_2 NPs have shown substantial antifungal potential, positioning them as promising agents for the control of various fungal infections. These nanoparticles exert their antifungal effects by disturbing the integrity of fungal cell membranes and interfering with essential cellular processes, including enzyme function and oxidative balance, ultimately leading to fungal cell death. MnO_2 NPs have shown strong inhibitory activity against several pathogenic fungi, particularly species of Candida and Aspergillus, which are commonly associated with human infections. The antifungal efficacy of MnO_2 NPs is largely attributed to their high surface area and their capability to generate oxygen species (ROS). The production of ROS induces oxidative stress, resulting in damage to fungal cell walls, membranes, proteins, and intercellular components, thereby suppressing fungal growth and proliferation. Moreover, MnO_2 NPs are being investigated for incorporation into antifungal coatings for medical devices, textiles, and agricultural materials, offering a sustainable and effective strategy for preventing fungal contamination and infection (Thatyana et al., 2023).

2.6.2 Photocatalytic Application

MnO_2 NPs are widely recognized for their remarkable photocatalytic activity, attributed to their high surface area, strong oxidative capability, and efficient charge transport properties. Upon light

irradiation. MnO_2 NPs generate reactive oxygen species (ROS), which play a critical role in the removal of various pollutants. This ability makes them kindly effectual in ecological remediation, particularly for the breakdown of organic contaminants such as dyes, pesticides, and industrial chemicals in wastewater. In addition to water treatments, MnO_2 NPs demonstrate photocatalytic activity against volatile organic compounds (VOCS) in air, contributing to air purification. Under light exposure, they facilitate the removal of microbial contaminants, heavy metals, and toxic substances by catalyzing their conversion into less harmful or more stable forms. This process provides an environmentally friendly and sustainable approach to pollution control. Furthermore, MnO_2NPs are being investigated for energy-related applications, including hydrogen production through photocatalytic water splitting, a promising pathway toward renewable energy generation. Owing to these multifunctional properties, MnO_2 NPs represent an important class of photocatalytic materials with broad applications in environmental protection, pollution mitigation, and energy conversion technologies (Chandra et al., 2025).

2.6.3 Adsorption Application

MnO_2 NPs exhibit significant potential in adsorption applications owing to their larger surface area, high structural reactivity, and strong oxidative properties. These characteristics enable them to efficiently remove heavy metals, synthetic dyes, and various organic pollutants from water and wastewater systems. The presence of active surface functional groups and favorable redox behavior facilitates the adsorption and immobilization of toxic contaminants such as arsenic, chromium, and lead, making MnO_2 NPs highly suitable for environmental remediation purposes. In addition to adsorption, MnO_2 NPs can catalytically degrade hazardous organic compounds, thereby enhancing overall pollutant removal efficiency. Their adaptability, environmental compatibility, and cost- effective synthesis, particularly through green approaches utilizing plant extract, further strengthen their relevance in sustainable water treatment and purification technologies (Ishfaq et al., 2023).

2.6.4 Energy Storage and Conservation Applications

Manganese dioxide is a chemical that has an essential role in the storage and conservation of energy. First of all, it is a component material for lithium-ion, zinc, carbon, and alkaline batteries. The reasons for this are its high capacity, long-lasting, and energy storage and release at a quick

rate. The feature that enables MnO_2 to perform such functions is its capability to undergo reversible redox processes. This is why it can also be used in energy storage devices like supercapacitors, where it can store energy quickly and release it at a fast rate. Moreover, researchers utilize manganese dioxide in making hydrogen storage systems. This is because MnO_2 acts as a catalyst in water splitting, thus increasing the hydrogen production, which can be used for energy conservation. Also, as a green material and cheap, MnO_2 is one of the best choices for sustainable energy storage technologies (Jiang et al., 2025).

CHAPTER THREE

3. MATERIALS AND METHODS

3.1 Chemicals and Apparatus

All the chemicals and reagents that were used for the preparation of MnO_2 nanoparticles were of analytical grade. Potassium permanganate ($KMnO_4$) was used as a precursor to synthesize the Mno_2NPs. Ferric chloride, Hydrochloric acid (HCl), Sulfuric acid (H_2SO_4), Ethanol (CH_3CH_2OH), Methanol (CH_3OH), Potassium bromide (KBr), Sodium Hydroxide (NaOH), Ammonia solution (NH_3), Wagner reagent, Benedict's solution, Iodine solution (I), Potassium Iodide (KI), and distilled water were also used.

Pipettes, measuring cylinders, Erlenmeyer flasks, furnace, funnels, filter paper, spatulas, an electrical grinding machine, beakers, aluminum foil, test tubes with a test tube rack, a mortar and pestle, droppers, an electronic beam balance, and a refrigerator were utilized. Additionally, characterization was performed using an X-Ray Diffraction (XRD), UV-Vis spectrometer, Fourier Transform Infrared spectroscopy (FT-IR), and a magnetic stirrer with a hot plate was also employed.

3.2 Collection and Preparation of Sample

The *Andrachne aspera* root was collected from the hills of East Shoa Oromia region, Wolanciti, Ethiopia. The collected *Andrachne aspera* root was thoroughly washed with distilled water to eliminate dirt particles and other impurities. Then *Andrachne aspera* root was dried in the shade at ambient temperature for one week under clean conditions. The dried *Andrachne aspera* root was pulverized with a mortar and pestle to produce a fine powder. The 15g of powder was mixed with 150mL distilled water and was refluxed for 1 hour at 70°C, until the aqueous extract mixture changed to brown. The end product was cooled to room temperature and filtered with Whatman filter paper. At the end extraction *Andrachne aspera* root helped society for antibacterial activity against disease-causing bacteria (Lung & Stegarescu, 2023).

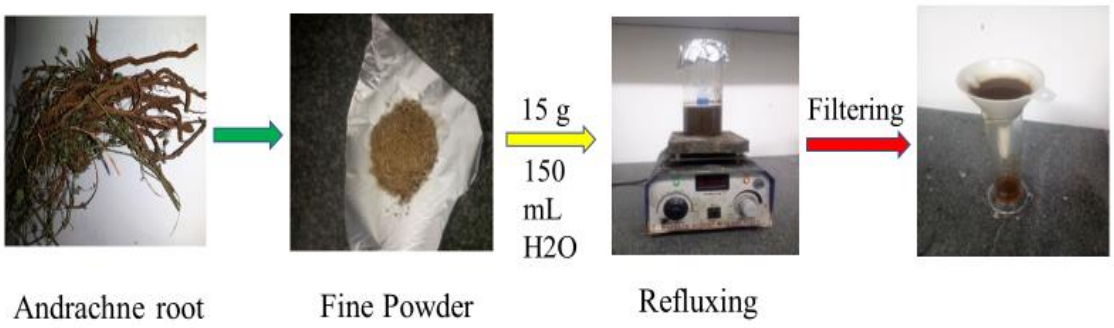

Figure 2: Plant Andrachane aspera root extraction

3.3 Synthesis of MnO_2 NPs Using *Andrachne aspera* Root Extract

Manganese dioxide nanoparticles were synthesized utilizing the root extract of Andrachne aspera in conjunction with potassium permanganate ($KMnO_4$) as the precursor at ambient temperature. The synthesis was conducted using volume ratios of 1:1, 1:2, and 2:1. For the 1:1 volume ratio synthesis, 50 mL of dilute root extract was mixed with 50 mL of 0.1 M $KMnO_4$ and stirred at ambient temperature for approximately 4h. To facilitate precipitate formation and maintain the pH of the suspension at approximately 11, 2 M sodium hydroxide (NaOH) was added, followed by an additional 30 minutes of stirring to ensure homogenous mixing of the base. Subsequently, the suspension was refrigerated at 4°C. The resulting mixture was centrifuged three times sequentially using ethanol, distilled water, and ethanol. The collected samples were dried in a laboratory oven at 80°C until ready for further processing. The synthesis procedures for the 1:2 and 2:1 volume ratio was conducted analogously, following the protocol established for the 1:1 ratio (Oliveira da Silva et al., 2024).

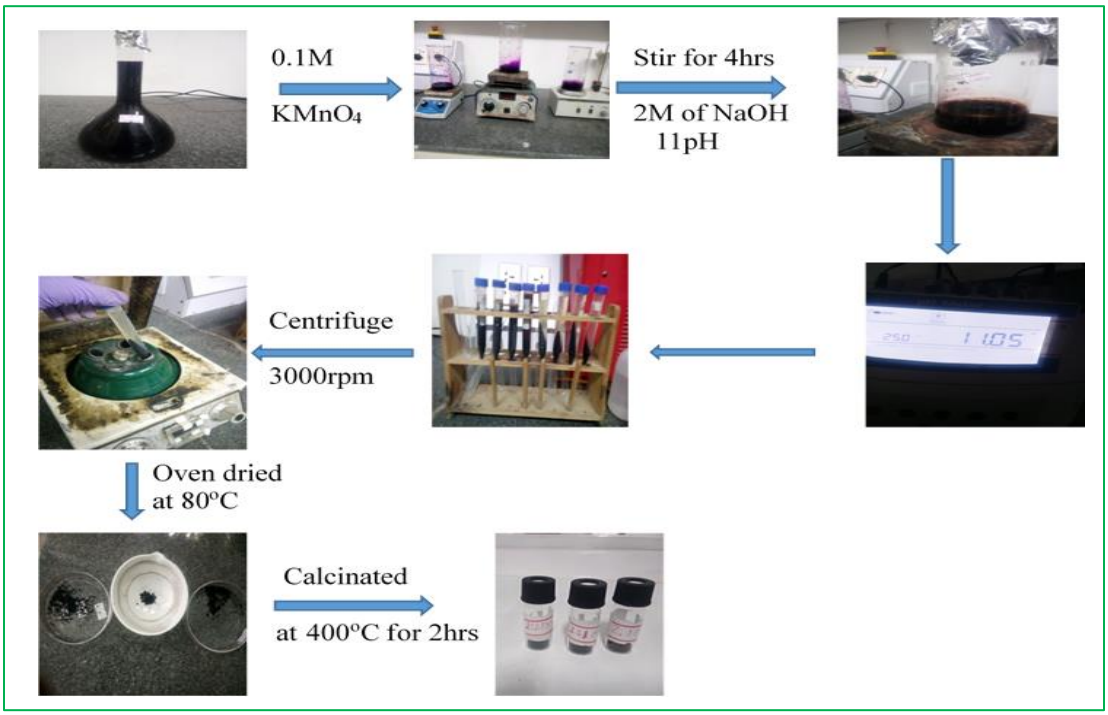

Figure 3: Schematic diagram of the synthesis of MnO_2 from andrachne aspera root

3.4 Phytochemical Tests

Test for Alkaloids

In a test tube with the extract, 1mL of 1% HCl was added. The mixture was cooked for 20 minutes, then cooled and filtered. Then, 1 mL of the filtrate will be tested with 0.5 mL Wagner's Test: Filtrates were treated with Wagner's reagent (Iodine in Potassium Iodide), and a brown/reddish precipitate was formed, indicating the presence of alkaloids.

Test for Flavonoids

Flavonoids were determined using the alkaline reagent test: The samples were sterilized with a few droplets of sodium hydroxide. The bright yellow colors generated, which turn colorless with the addition of dilute acid, suggest the existence of flavonoids.

Test for Phenols

Ferric Chloride Test Method: The botanical extracts were mixed with water and warmed. To this, two milliliters of ferric chloride solution were added, and the color was brown, not green or blue. The results were negative, indicating that the phenols were not present.

Test for Glycosides

Keller-Killani Test: Approximately 0.5 mL from every single extract was collected and subjected to the following tests: 1 mL of glacial acetic acid with trace amounts of ferric chloride and 1 mL of concentration. Sulphuric acid was added to the extract, resulting in a dark hue, but no layers formed in the formation of glycosides.

Test for Saponins

Froth test: 0.2 g of extract was cooked in 2mL of distilled water on a hotplate and then filtered. A 1mL portion of aqueous filtrate will be combined with 2mL of distilled water and aggressively shaken to produce a stable, persistent foam. The foam was combined with approximately three drops of olive oil and vigorously shaken. An emulsion created confirms the existence of saponins.

Test for Steroids

Steroids were examined using the procedures of Alhadi et al. (2015). One milliliter of extract was mixed in 10 mL of chloroform, and the walls of the test tube were coated with an equal amount of concentrated H2SO4. The upper layer was colored red, whereas the H2SO4 layer exhibited yellow with green fluorescence. This suggests the existence of steroids.

Reducing Sugar

This test employs Fehling's method (Fehling A and Fehling B). Fehling A is a deep blue aqueous solution of copper (II) sulfate, whereas Fehling B is an opaque solution of potassium sodium tartrate (Rochelle salt) that has been rendered excessively alkaline with sodium hydroxide. When heated with reducing sugar, it produces a brick-red precipitate, which confirms the existence of reducing sugars. Fehling's test is a chemical test that detects the presence of reducing sugars. It entails reacting a sample with Fehling's solution, a blue solution containing copper (II) ions, to examine if a brick-red precipitate of copper(I) oxide appears, indicating a positive result; however,

in a phytochemical test for Andrachne aspera, a blue precipitate was obtained rather than brick red.

3.5 Characterization Technique

The band gap energy and optical properties of biosynthesized MnO_2 NPs were characterized by a UV-Vis diffuse reflectance spectrophotometer (Elico SL, 150) at the Material Science Department, Adama University, over a wavelength range of 200–800 nm. The crystal-like shape of the MnO_2 NPs was ascertained by X-ray diffraction (XRD) with a Shimadzu XRD-700 diffractometer at the Material Science Department, Adama Science and Technology University. The data were collected using Cu K radiation (= 1.5406) at an accelerated voltage of 40 kV, and the deflection prefigures were noted over the 2θ range of 10 to 80 at a scan rate of 28 20/min. FTIR spectroscopy was operated utilizing a Thermo Scientific Nicolet iS50 spectrometer at the Chemical Engineering Department, Addis Ababa Science and Technology University. The spectra were captured from 4000 to 400 cm-1 with a step size of 16 cm-1 to ascertain the chemical bonding groups on the surface of the ZnO NPs that caused reduction, stabilization, and capping. Additionally, thermogravimetric analysis (TGA) of the green fabrication MnO_2 NPs was performed at the Department of Materials Science, Adama University. The TGA was operated in a nitrogen atmosphere with a flow rate of 50 mL/min, capturing thermograms from 25 to 800 °C at an elevated temperature of 20 °C/min to block oxidation and investigate the sample's thermal degradation behavior under inert conditions.

3.6 Procedures for Antibacterial Activity

The antibacterial efficacy of biosynthesized manganese dioxide (MnO_2), prepared using potassium permanganate ($KMnO_4$) precursor and Andrachne aspera root extract in ratios of 1:1, 2:1, and 1:2, was evaluated against four bacterial strains: Staphylococcus aureus, Streptococcus pyogenes, Escherichia coli, and Pseudomonas aeruginosa. These bacterial strains were sourced from the Microbiology Laboratory of Adama Science and Technology University. The antibacterial activities of the bio-fabricated MnO_2 nanoparticles were assessed employing the disc diffusion process.

3.6.1 Preparation of Inoculum

Four test pathogens were cultured overnight in Mueller-Hinton broth (MHB) until achieving a 0.5 McFarland turbidity standard. Bacterial strains were engineered to have 1.5 ×10^8 colony forming units (CFU/ml). To count bacteria, a 0.5 McFarland standard was generated by blending 0.05ml of 1% $BaCl_2$ and 9.95ml of 1% H_2SO_4 in purified water. To compare the microbial mixture, the formulation was placed against a Wickerham card to see how turbid the cultures were. Subsequently, 100 µL of each test pathogen was uniformly spread onto Mueller-Hinton agar (MHA) plates.

3.6.2 Disc Diffusion Method for Antibacterial Activity

Bacterial isolates of clinical origin were acquired from the American Type Culture Collection (ATCC) and were used for the investigation of the antibacterial effect of the synthesized NPs. The strains are Escherichia coli (ATCC 25922), Pseudomonas aeruginosa (ATCC 27853), Streptococcus pyogenes (ATCC 19615), and Staphylococcus aureus (ATCC 25923). A 0.5 McFarland standard was composed by blending 99.95 mL of 1% H_2SO_4 with 0.048 mL of 1% BaCl in distilled water. The bacterial suspension was tuned to this turbidity standard, which indicates a bacterial concentration of approximately 1.5 10 CFU/mL, and verified at 625 nm by a UV-Vis spectrophotometer. The disk diffusion technique was utilized to find out the antimicrobial activity. The fabricated nanoparticles were dissolved in DMSO to prepare 100, 50, 25, and 12.5 mg/mL solutions. The bacterial cultures were adjusted to a 0.5 McFarland standard and then evenly spread onto Mueller-Hinton agar plates utilizing a sterile cotton swab. The plates were left to dry for 10 to 30 minutes. Sterile paper disks were immersed in each nanoparticle concentration, allowed to dry, and then placed on the agar plates inoculated with bacteria. The following incubation was conducted at 35 °C for 24 h. Every test was repeated three times. A ciprofloxacin disk (30 g) was utilized as a standard control. The areas showing microbial suspension were read with a digital antibiotic zone reader.

CHAPTER FOUR

4. RESULTS AND DISCUSSION

4.1 Characterization of MnO_2 NPs

4.1.1 Phytochemical Analysis

Table 2: Results for phytochemical test

Tests	Positive	Negative
Alkaloids	✓	
Flavonoids	✓	
Saponins	✓	
Steroids	✓	
Phenol		✓
Glycoside		✓
Reducing Sugar		✓

Figure 4: Phytochemical test result

4.1.2 UV–Vis Diffuse Reflectance Spectroscopy (DRS) Analysis

The optical properties and band gap energies of the biosynthesized MnO_2 NP were investigated using UV-Vis Diffuse Reflectance Spectroscopy (DRS), and the obtained spectra are presented in Figures 5 (a, b, and c) for MnO_2 NP synthesized with 1:1, 2:1, and 1:2 ratios, respectively. All samples exhibited strong reflectance between 200 and 800 nm, characteristic of materials with efficient light scattering properties. Distinct absorption features were observed in the ultraviolet region, specifically around 250-300 nm, indicating electronic transitions within the MnO_2 structure.

Tauc plots were used to assess optical band gap energy utilizing the Kubelka-Munk function, F(R) = (1−R)2/(2R), wherein R represents reflectance. The indirect band gap energies were estimated by extrapolating the linear portion of the plots of $[F(R)h\nu]^2$ against photon energy (hν) to the x-axis, where $[F(R)h\nu]^2 = 0$. The calculated band gap energies were found to be 2.7 eV for the 1:1 MnO_2 NP, 2.6 eV for the 2:1 MnO_2 NP, and 2.8 eV for the 1:2 MnO_2 NP formulations. Among the three MnO_2 nanoparticle ratios, the 1:2 volume ratio exhibits the highest band gap energy. This suggests that the band gap energy of MnO_2 nanoparticles is strongly dependent on particle size. Specifically, smaller particle sizes correspond to larger band gap energies. This phenomenon can be explained by the quantum confinement effect. As particles shrink to nanometer dimensions, orbital interactions between atoms become limited, leading to narrower energy bands. Consequently, the separation between the conduction and valence bands increases, resulting in an enlarged band gap energy. The observed band gaps are consistent with reported values for semiconductor metal oxides, suggesting their potential for various applications (Matsui et al., 2024). The high reflectance throughout the visible spectrum also implies a light-colored appearance for these materials.

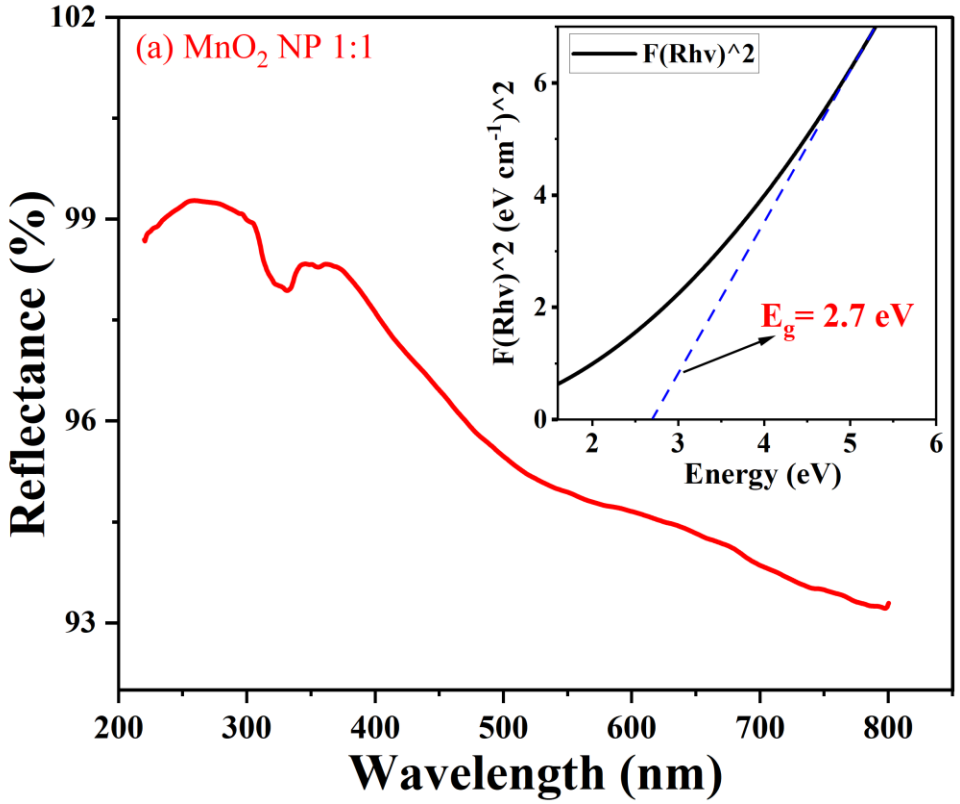
(a) MnO2 NP 1:1
Reflectance (%)
Wavelength (nm)
F(Rhv)^2
F(Rhv)^2 (eV cm-1)^2
Energy (eV)
Eg= 2.7 eV

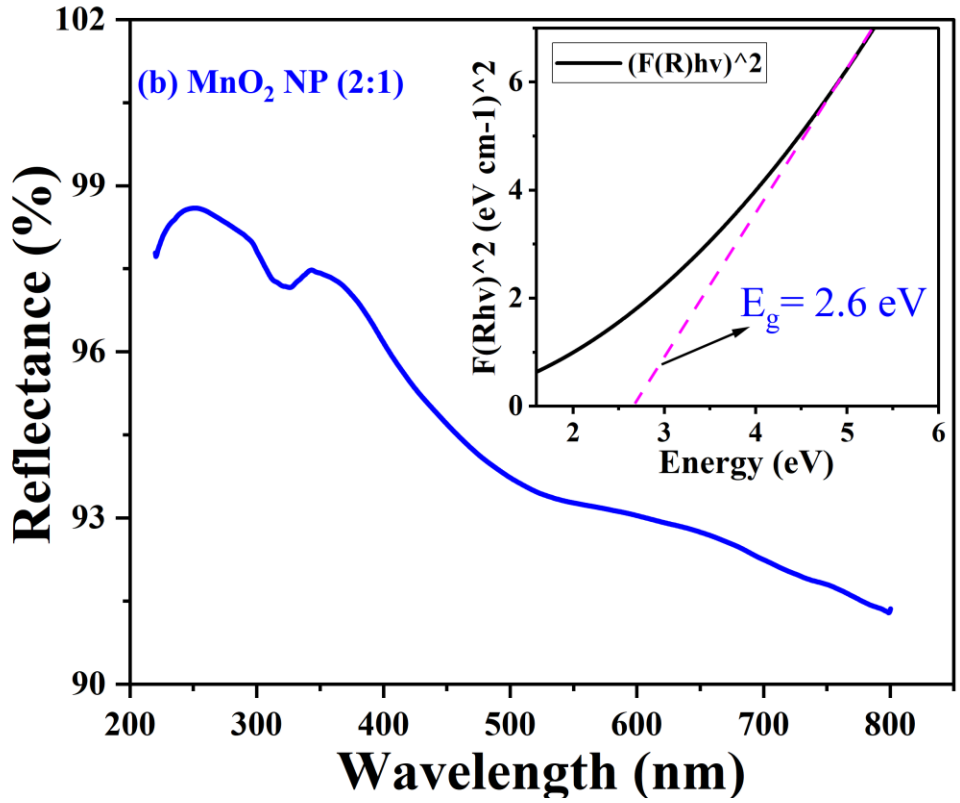
(b) MnO2 NP (2:1)
Reflectance (%)
Wavelength (nm)
(F(R)hv)^2
F(Rhv)^2 (eV cm-1)^2
Energy (eV)
Eg= 2.6 eV

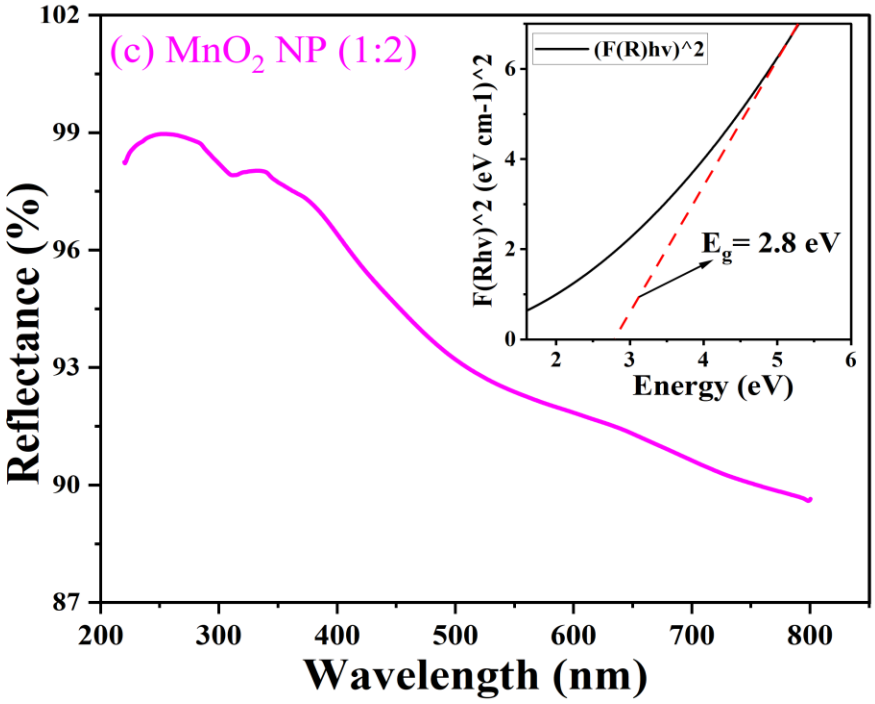

Figure 5: UV–Vis diffuse reflectance spectra (DRS) and corresponding Tauc plots of (a) MnO2 NP (1:1), (b) MnO2 NP (2:1), and (c) MnO2 NP (1:2), along with their respective band gap energies.

4.1.3 X-ray Diffraction (XRD) Analysis

X-ray Diffraction (XRD) was used to examine the crystal structure and phase purity of the prepared MnO_2 NPs. Using three different ratios between the metal and plant extract, as prepared samples of 1:1, 2:1, and 1:2, respectively, were produced. All three samples demonstrated similar peak position and distribution of peak intensity (Fig 6(a-c)). This shows that the phase formation was consistent across different synthesis conditions. The sharp and well-defined peaks also show the production of crystalline MnO_2 NPs. All samples show the major diffraction peaks can be indexed to the planes (001), (200), (211), (301), and (202), which are characteristic of the birnessite form of MnO, and the patterns obtained agree with the standard JCPDS card number 96-900-1272. From this, it can be deduced that a pure MnO phase has been produced without any contamination from secondary phases or impurities. This is an extremely positive step because it proves that MnO_2 NPs can be produced using a green synthetic method with high crystallinity and purity.

Meanwhile, the crystal size of the produced material was determined using Scherrer's equation (below).

$$\boldsymbol{D = \frac{k\lambda}{\beta cos\theta}} \qquad 1$$

where D is the size of the crystal, λ is the X-ray wavelength, β is the full width at half maximum (FWHM) intensity of the peak [rad], and θ is the Bragg's angle of diffraction. The Debye-Scherrer equation was utilized to assess the crystallite size of the produced MnO_2 NPs. The FWHM of the most intense diffraction peak was considered. The calculated crystallite sizes for the 1:1, 2:1, and 1:2 metal-to-extract ratios were obtained to be 28.58 nm, 28.83 nm, and 25.83 nm, separately. The slightly smaller crystallite size observed for the 1:2 sample suggests that increasing the amount of plant extract may enhance the capping and stabilizing effect during nanoparticle formation, thereby limiting crystal growth. This suggests that the plant extract functions both as a reducing agent and as a stabilizer, controlling particle size and enhancing nanoparticle stability.

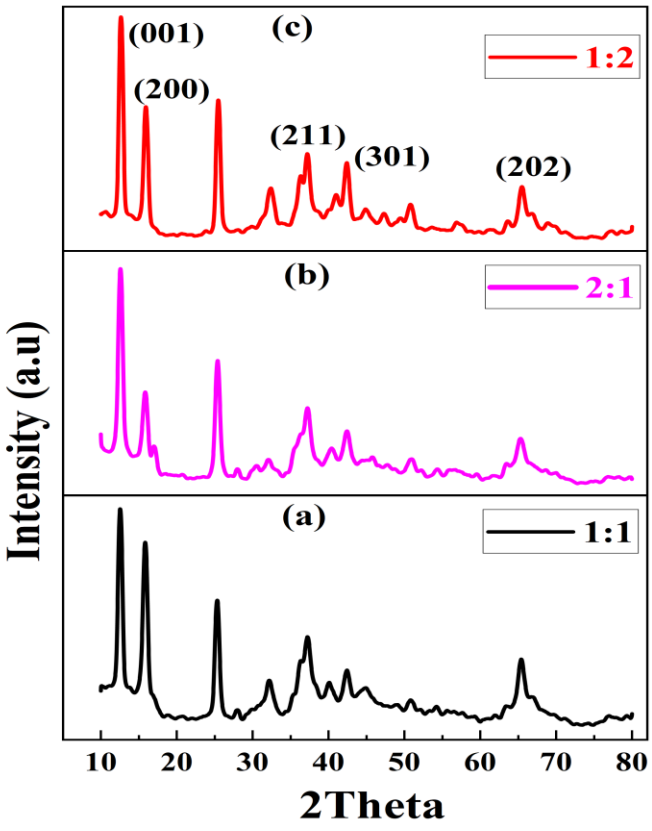

Figure 6: XRD patterns of biosynthesized MnO_2 NPs using: (a) 1:1, (b) 2:1, and (c) 1:2 mass ratio of manganese precursors to plant extract.

Table 3:Crystallite sizes of Biosynthesized MnO_2 NPs.

Sample name	2Theta	FWHM	Crystal size (D) nm	Average D (nm)
MnO_2 NP (1:1)	12.70	0.2800	28.55	28.58
	16.01	0.2400	33.43	
	25.45	0.2800	29.09	
	32.31	0.2000	41.35	
	37.30	0.3600	23.29	
	42.46	0.2800	30.44	
	65.50	0.6800	13.89	
MnO_2 NP (2:1)	12.60	0.2400	33.3	28.83
	15.88	0.4000	20.05	
	17.06	0.2000	40.17	
	25.37	0.4400	18.51	
	37.22	0.6400	13.1	
	42.46	0.4800	17.76	
	65.10	0.1600	58.9	
MnO_2 NP (1:2)	12.68	0.2000	39.97	25.83
	15.98	0.2000	40.11	
	25.47	0.2800	29.09	
	32.27	0.4000	20.68	
	36.29	0.4400	19	
	37.19	0.3600	23.28	
	42.42	0.5200	16.39	
	65.48	0.5200	18.16	

4.1.4 Fourier Transform Infrared (FTIR) Analysis

FTIR spectroscopy was employed to reveal the functional groups in the Andrachne aspera root extract, which are probably involved in reducing manganese precursors and stabilizing the

produced NPs, besides confirming the formation of MnO_2 NPs. Figure 7 shows the FTIR spectra of (a) andrachne aspera root extract and (b) bio, fabricated MnO_2 NPs.

The FTIR spectrum of the plant root extract (Figure 7a) shows several strong absorption bands indicating the presence of various phytochemicals. A wide and strong absorption band located at 3272 cm^{-1} is explained by O-H stretching vibrations typically existing in hydroxyl groups of alcohols, phenols, or carboxylic acids, the functional groups well-known for their reducing power in green synthesis. A sharp peak at 1738 cm^{-1} is due to the C=O stretching band, which might be from carboxylic acids or ester groups. Moreover, the band at 1614 cm^{-1} is credited either to C=O stretching of amides or to C=C stretching of aromatic rings. Other peaks at 1368 cm^{-1} (C-H bending) and 1020 cm^{-1} (C-O stretching characteristic of alcohols or polysaccharides) validate the phytochemical richness of the plant root extract and its capability to serve as bioagents during nanoparticle generation.

In contrast, the FTIR spectrum of the bio-synthesized MnO_2 NPs (Figure 7b) reveals several shifts and new bands, providing evidence for the formation of the interaction between the manganese precursor and the biomolecules present in the plant extract. The broad O-H band at 3212 cm^{-1}, displayed as red, shifted from the extract, provides evidence for hydrogen bonding or coordination between hydroxyl groups and the surface of the nanoclusters. The band at 1644 cm^{-1}, likely reflects the bending vibration of the water molecules adsorbed to the MnO surface or residual organics. The band at 1383 cm^{-1} may be due to bending C-H modes or symmetric stretching of surface in-phase carboxylate groups. Most importantly, the strong absorption band at 441 cm^{-1} with a corresponding peak at 892 cm^{-1} is attributed to Mn-O and Mn-O-Mn stretching vibration modes, providing evidence for MnO_2 NPs. Collectively, these bands provide evidence for MnO_2 NPs. The presence of bands reflective of carbon-based functional groups in the MnO spectrum suggests that organic molecules from the plant extract are adsorbed on the surface of the MnO_2 NPs, functioning as both reducing agents, converting Mn^{+2} to Mn^{+4}, and as capping and stabilizing agents, which prevent agglomeration through surface functionalization.

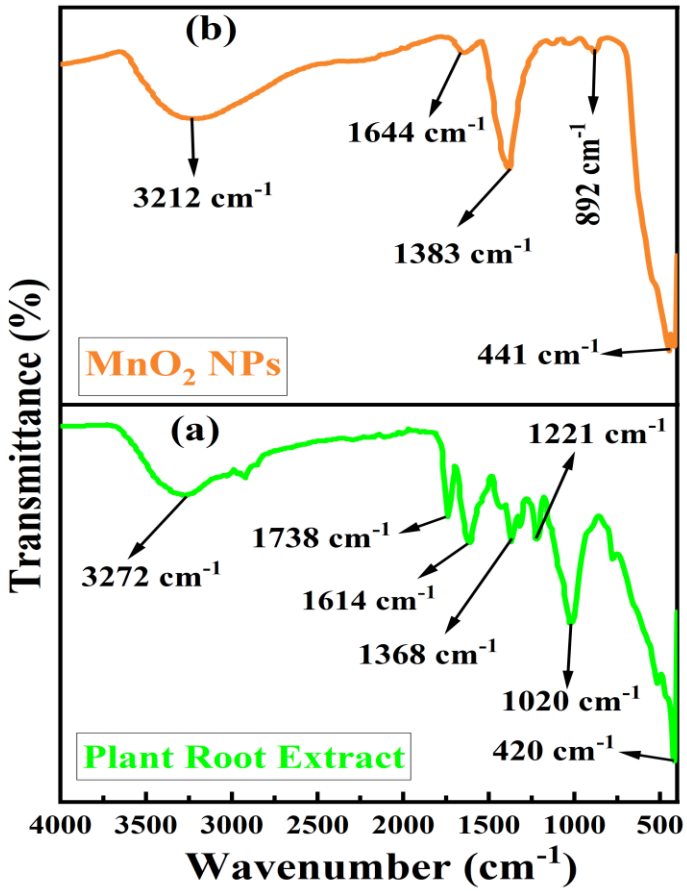

Figure 7: FTIR Spectra of (a) Andrachne aspera root extract, (b) MnO_2 nanoparticles

4.1.5 Thermogravimetric Analysis of Biosynthesized MnO_2 NPs

The thermal analysis of biosynthesized MnO_2 NPs was carried out using TGA and DTA techniques, as shown in Figure 8. The thermogram was recorded from room temperature to 800 °C under a nitrogen atmosphere on a DTG-60H instrument with a load of 8.567mg. The TGA thermogram (black line) at left side indicates three major weight loss regions. The initial weight loss of 1.15% at 66.88 °C was observed and assigned due to the dehydration of moisture and physically adsorbed water molecules present on the surface of nanoparticles. The next weight loss of 0.65% was observed between 201 °C and 265 °C, associated with the decomposition of residual organic molecules, such as phytochemicals originating from plant extract used during bio-production. The organic molecules may have been partially adsorbed on the surface of MnO_2 NPs, and act as capping and stabilizing agents. A third weight loss of 0.57% was measured gradually

between 265 °C and 450 °C, and it is attributed to the removal of more strongly bound organic moieties or to structural reorientations within the MnO lattice. Beyond 450 °C, the TGA value plateaued, however, providing evidence for no further weight loss. This suggests the current application of the photosynthesized MnO_2 NPs to be thermally stable up to 800 °C. This confirms the current application of the green-synthesized MnO_2 NPs to be thermally robust at high temperatures. The DTA tests (red line) at the right side of the curve confirm the TGA results. It shows three exothermic peaks corresponding to the weight loss steps, observed distinctly at 66.88 °C, 201 °C, and 265 °C, respectively. No clear, sharp endothermic or exothermic peaks were observed at the high temperature (>300 °C) related to nanoparticles. Overall, the minimal weight loss and steady TGA/DTA profile demonstrate that the MnO_2 NPs synthesized via the green synthesis exhibit excellent thermal stability. The decomposition behavior further confirms the presence of surface-bound organic groups, which play a vital function in NP stabilization. These conclusions are consistent with earlier reports on the thermal analysis of biosynthesized metal oxide nanoparticles.

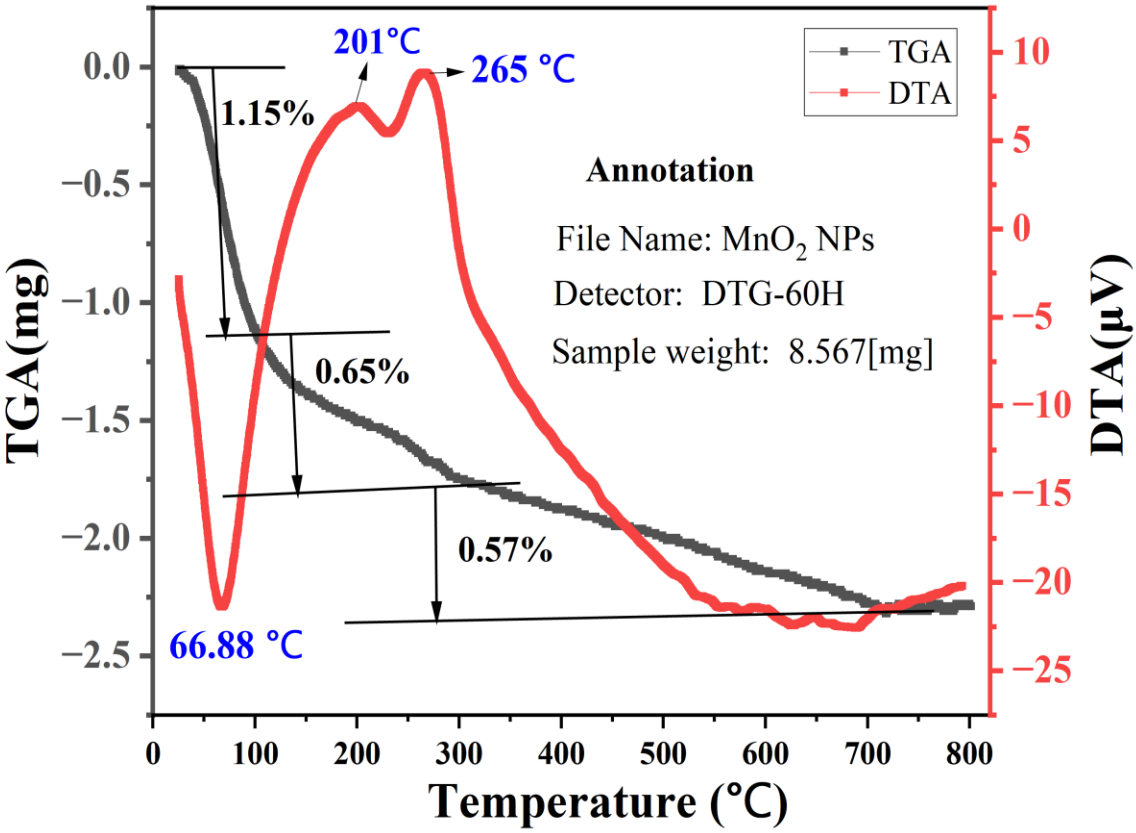

Figure 8: TGA and DTA thermograms of biosynthesized MnO_2 nanoparticles.

4.2 Antibacterial Activity of Biosynthesized MnO_2 Nanoparticles

Antibacterial Properties of MnO_2 Nanoparticles

Manganese dioxide nanoparticles have excellent antibacterial actions and, therefore, are interesting for biomedical applications. The treatment of bacteria with MnO_2 NPs leads to the production of generated ROS and induces oxidative stress that damages key cellular components (membranes, proteins, and DNA). The nanoparticles may also damage bacterial cell membranes by direct contact and would eventually cause leakage and bacterial cell death. Moreover, released Mn^{2+} ions can interfere with key processes in bacterial metabolism. Thanks to the small size of the MnO_2 NPs, they are strongly attracted to the negatively charged bacterial membranes and have a large attachment and penetration.

Mechanisms of Antibacterial Action

MnO_2 NPs have antibacterial effects by a number of biodiversity mechanisms, which, in combination, result in the destruction of bacterial cells. A key mechanism is the production of reactive oxygen species (ROS) such as superoxide anions, hydroxyl radicals, and hydrogen peroxide. These ROS induce oxidative stress, whereby the vital cellular components, such as proteins, lipids, and DNA, are damaged, leading to bacterial cell death. Furthermore, MnO2 nanoparticles may damage bacterial cell membranes by direct physical contact since they are of nanoscale sizes and have high surface reactivity. This interaction compromises membrane integrity, increases permeability, and leads to the leakage of vital intracellular contents, disrupting cellular function. Moreover, MnO_2 nanoparticles can release manganese ions (Mn^{2+}) under physiological conditions. These ions can enter bacterial cells and interfere with key biological processes such as enzyme activity, DNA replication, and nutrient transport. Electrostatic interactions between the typically negatively charged bacterial surfaces and the surface charge of MnO_2 NPs further enhance their adhesion to bacterial cells, increasing the efficiency of ROS generation and membrane disruption. These combined effects also inhibit bacterial metabolism, including ATP synthesis and protein production, leading to cell death. Overall, the antibacterial action of MnO_2 nanoparticles is driven by a synergistic effect of oxidative damage, ion toxicity, membrane disruption, and metabolic interference, making them highly effective against a broad range of bacterial pathogens.

In addition, MnO can release Mn (II) ions in vivo, which are capable of penetrating bacterial cells and downregulating enzyme activities, DNA replication, and nucleic acid transport. The positive charge of the bacterial surface (which is negative in nature) and the surface of the MnO_2 NPs leads to strong electrostatic attractions, resulting in positioning and subsequent bacterial cell surface interactions. The most notable effect of MnO_2 NPs will then be the efficient generation of ROS, along with direct interactions with membranes, which result in the breakage and leakage of cellular contents and inhibition of metabolism. Overall, the antibacterial action of MnO_2 nanoparticles is driven by a synergistic effect of oxidative damage, ion toxicity, membrane disruption, and metabolic interference, making them highly effective against a broad range of bacterial pathogens.

The antibacterial potential of MnO_2 nanoparticles synthesized via a green route was evaluated against four clinically relevant bacterial strains: *Escherichia coli*, *Pseudomonas aeruginosa*, *Staphylococcus aureus*, and *Streptococcus pyogenes* through the disk diffusion method. Positive control (25 μg) antibiotics) and DMSO were used as positive and negative controls, respectively. The study investigated three different precursor molar ratios, MnO_2 (1:1), MnO_2 (2:1), and MnO_2 (1:2), at four dilution levels: 100, 50, 25, and 12.5 mg/mL. The reticence areas were recorded in millimeters and compared with a positive control (PC, standard antibiotic) and a negative control (NC, distilled water). As illustrated in Figures 9, 10, and 11 below. The antibacterial activity of MnO_2 NPs was matched with the positive control, Ampicillin: the results indicate that the nanoparticles exhibited clear zones of inhibition against all tested strains, with larger zones observed at higher concentrations, confirming a dose-dependent antibacterial effect. MnO_2 NPs synthesized by using the (1:2) ratio for all concentrations showed high antibacterial activity against all bacterial strains compared to (1:1) and (2:1) ratios. This is most probably due to the small size it possessed compared to others, which led to high penetration ability and caused fast cell damage. Moreover, as the concentration of nanoparticles increased, the antibacterial activity of these nanoparticles was also enhanced, similar to the previous report.

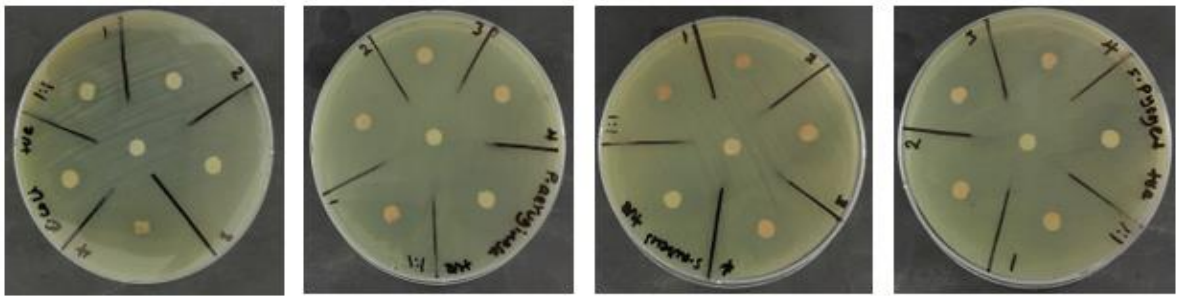

Figure 9: Photographs of antibacterial activities of MnO_2 (1:1) ratio NPs

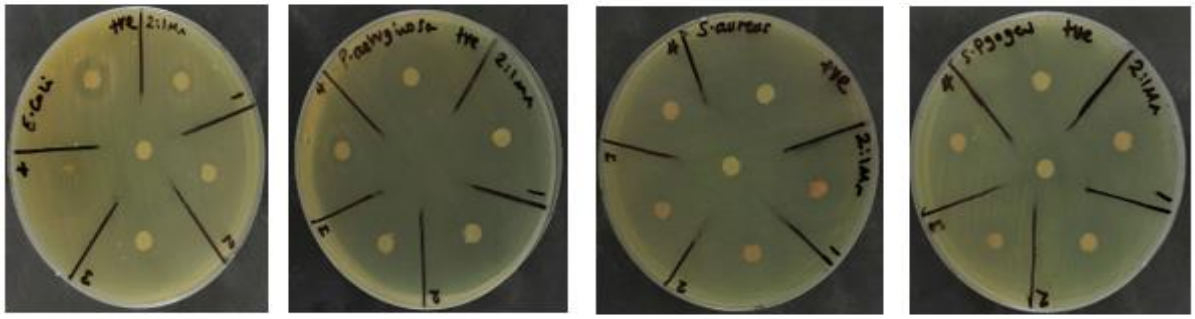

Figure 10: Photographs of antibacterial activities of MnO_2 (2:1) ratio NPs

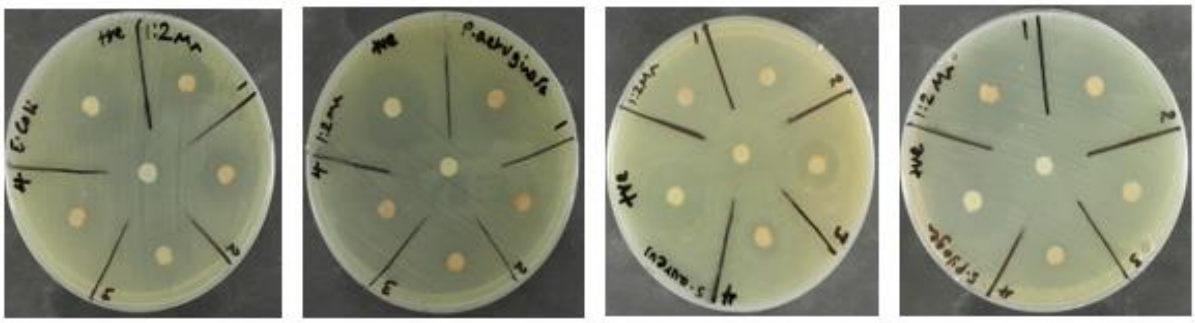

Figure 11: Photographs of antibacterial activities of MnO_2 (1:2) ratio NPs

Table 4: Results of dilution and zone of clearance in mm for bio-synthesized different ratios of MnO_2 NPs

NPs and Organisms		**Dilution Results, Means of three replications, and Inhibition zones in mm**					
NPs	Test Organism	100 mg/mL	50 mg/mL	25 mg/mL	12.5 mg/mL	PC (+ve)	NC (-ve)
MnO_2 (1:1)	E. coli	14	11	8.5	7.5	20	6
	P. aeruginosa	14.5	11.5	9.5	8	21	6
	S. aureus	16	13.5	10.5	8.5	19.5	6
	S. pyogenes	14.5	12.5	9.5	8	19	6
MnO_2 (2:1)	E. coli	15.5	13.5	10.5	9.5	20	6
	P. aeruginosa	16.5	14.5	12.5	11	21	6
	S. aureus	17	14	11.5	9.5	21.5	6
	S. pyogenes	15.5	13.5	10	8.5	20	6
MnO_2 (1:2)	E. coli	15	13.5	12	9.5	22.5	6
	P. aeruginosa	16.5	14	11	8.5	21	6
	S. aureus	18	16.5	11.5	9	20.5	6
	S. pyogenes	18.5	16	12.5	10.5	21.5	6

The antibacterial activity results presented in Table 3 above revealed a clear dose-dependent relationship across all MnO_2 NPs formulations and tested bacterial strains. As the concentration of MnO_2 NPs decreased from 100 to 12.5 mg/mL, a corresponding decline in inhibition zone diameter was observed, indicating reduced antibacterial efficacy at lower concentrations. At 100 mg/mL, the highest activity was recorded, with inhibition zones ranging from 14.0 to 18.5 mm across all strains and formulations. Conversely, at the lowest tested concentration (12.5 mg/mL), inhibition zones decreased to between 7.5 and 10.5 mm, though antimicrobial effects remained detectable. Among the three nanoparticle formulations, MnO_2 NPs (1:2) exhibited the strongest antibacterial properties, especially versus Gram-positive strains such as *S. aureus* (18.0 mm) and *S. pyogenes* (18.5 mm) at 100 mg/mL. This enhanced performance may be attributed to higher crystallinity or increased surface reactivity, possibly due to the greater proportion of the reducing/stabilizing agent

used during synthesis. MnO_2 NPs (2:1) also demonstrated considerable antibacterial effectiveness, with inhibition zones reaching 16.5-17.0 mm, mainly against *P. aeruginosa* and *S. aureus*. The improved movement in this formulation could be due to a higher concentration of the metal precursor, potentially resulting in smaller and more reactive particles. In comparison, MnO_2 NPs (1:1) showed slightly lower antibacterial activity, with inhibition zones of 14.0-16.0 mm at the highest concentration, though it remained effective across all tested strains. The sensitivity of different bacterial strains to MnO_2 NPs was found to vary also according to their Gram classification. Results revealed that Gram-positive bacteria (S. aureus and S. pyogenes) are more susceptible to MnO_2 NPs than gram, negative bacteria (E. coli and P. aeruginosa). The difference in the cell walls of the bacterial strains probably led to the distinct reactivity of these strains. The thick peptidoglycan of the Gram-positive bacterial cell wall may be more susceptible to nanoparticle, induced oxidative stress and penetration. By serving as a structural defense, the outer membrane in Gram-negative bacteria hinders nanoparticle penetration and lowers their antimicrobial performance (Zhydzetski et al., 2025).

Control experiments validated the observed antibacterial activity. The positive control (standard antibiotic) exhibited inhibition zones between 19.0 and 22.5 mm, confirming its effectiveness. The negative control (distilled water or DMSO) showed no inhibition (6 mm, equal to the well diameter), indicating that the antimicrobial effects were solely due to the MnO_2 NPs. Lastly, the study confirms that biosynthesized MnO_2 NPs possess significant antibacterial properties, which are strongly influenced by both synthesis ratio and concentration, with a higher concentration of the metal precursor potentially resulting in smaller and more reactive particles. The MnO_2 NPs (1:2) formulation demonstrated the most potent activity overall, underscoring the importance of optimizing synthesis conditions to enhance nanoparticle bioactivity. These discoveries support the capacity of bio-fabrication MnO_2 NPs as promising alternatives to conventional antimicrobial agents in medical and environmental applications.

CHAPTER FIVE

5. CONCLUSION AND RECOMMENDATION

5.1 Conclusion

This investigation effectively achieved the synthesis of MnO_2 nanoparticles utilizing Andrachne aspera root extract via a green synthesis method characterized by its environmental sustainability and cost-effectiveness. The phytochemical constituents in the extract served as natural bio-agents, facilitating the formation of stable and well-defined MnO_2 NPs. Fourier-transform infrared spectroscopy verified bioactive compounds- nanoparticle surfaces interaction, while X-ray diffraction shows that the analysis validated the crystalline shape and phase integrity of the synthesized NPs. Thermogravimetric analysis demonstrated thermal stability of the nanoparticles up to 450 °C, indicating their potential applicability in high-temperature environments. Notably, the green production of MnO_2 NPs displayed pronounced antibacterial efficacy against both Escherichia coli and Staphylococcus aureus, underscoring their promise as potent antimicrobial agents. This investigation not only substantiates the feasibility of employing biosynthetic routes for scalable MnO_2 NPs production but also highlights the growing importance of plant-mediated nanotechnology within biomedical and environmental domains. The findings suggest that MnO_2 NPs synthesized via Andrachne aspera root extract represent a viable alternative for the expansion of innovative antibacterial materials, thereby adding to progress in the fields of nanotechnology and green chemistry.

5.2 Recommendations and Future Work

This study demonstrates the successful bio-synthesis of MnO_2 NPs with the Andrachne aspera root extract, and also their antibacterial properties have been identified. It may be further enhanced through an assortment of possible future experiments:

- Clarify the biochemical mechanisms and identify the specific phytochemicals that contribute to the reduction and stabilization of NPs.
- Tune synthesis parameters such as pH, temperature, time of reaction, and ratios of precursors to increase the production, uniformity, and functionality of MnO_2 NPs.
- Study the embedding of MnO_2 NPs in composite materials for different uses.
- Extend the antibacterial study to more bacterial strains.

REFERENCES

Ahmed, K. H., Zuria, A. M., & Mohamedi, M. (2025). Integration of Carbon Nanotubes into Manganese Dioxide Nanorods for Enhanced Enzymeless Electrochemical Glucose Sensing with High Sensitivity and Selectivity. *Biosensors*, *15*(4). https://doi.org/10.3390/bios15040215

Aigbe, U. O., & Osibote, O. A. (2024). Green synthesis of metal oxide nanoparticles and their various applications. *Journal of Hazardous Materials Advances*, *13*, 100401. https://doi.org/https://doi.org/10.1016/j.hazadv.2024.100401

Al-Harbi, N., & Abd-Elrahman, N. K. (2025). Physical methods for preparation of nanomaterials, their characterization and applications: a review. *Journal of Umm Al-Qura University for Applied Sciences*, *11*(2), 356–377. https://doi.org/10.1007/s43994-024-00165-7

Altammar, K. A. (2023). *A review on nanoparticles : characteristics, synthesis, applications, and challenges*. *April*, 1–20. https://doi.org/10.3389/fmicb.2023.1155622

Asfaw, A., Lulekal, E., Bekele, T., Debella, A., Meresa, A., Sisay, B., Degu, S., & Abebe, A. (2023). Antibacterial and phytochemical analysis of traditional medicinal plants: An alternative therapeutic Approach to conventional antibiotics. *Heliyon*, *9*(11), e22462. https://doi.org/https://doi.org/10.1016/j.heliyon.2023.e22462

Chai, L., Chen, H., Yang, X., Liu, J., Yang, Q., Huang, S., Tang, M., Zhu, X., Li, H., Zhang, Y., & Liu, M. (2026). MnO2 nanozyme-based ratiometric fluorescent nanoplatform for glutathione detection and intracellular imaging. *Talanta*, *297*, 128645. https://doi.org/https://doi.org/10.1016/j.talanta.2025.128645

Chandra, S., Pandit, S., Gupta, A., Sahni, M., Rajeev, M., & Fosso-Kankeu, E. (2025). Sustainable Mn-doped ZnO Nanoparticles as an Efficient Cathode Catalyst for Enhanced ORR and Photocatalytic Dye Degradation in Microbial Fuel Cells. *Water, Air, & Soil Pollution*, *236*(13), 835. https://doi.org/10.1007/s11270-025-08474-1

Corrales, J., Acosta, J., Castro, S., Riascos, H., Serna-Galvis, E., Torres-Palma, R. A., & Ávila-Torres, Y. (2022). Manganese Dioxide Nanoparticles Prepared by Laser Ablation as Materials with Interesting Electronic, Electrochemical, and Disinfecting Properties in Both Colloidal Suspensions and Deposited on Fluorine-Doped Tin Oxide. *Nanomaterials*, *12*(22). https://doi.org/10.3390/nano12224061

Du, T., Chen, S., Zhang, J., Li, T., Li, P., Liu, J., Du, X., & Wang, S. (2020). Antibacterial activity of manganese dioxide nanosheets by ros-mediated pathways and destroying membrane integrity. *Nanomaterials*, *10*(8), 1–14. https://doi.org/10.3390/nano10081545

Eker, F., Duman, H., Akdaşçi, E., Bolat, E., Sarıtaş, S., Karav, S., & Witkowska, A. M. (2024). A Comprehensive Review of Nanoparticles: From Classification to Application and Toxicity. In *Molecules* (Vol. 29, Issue 15, p. 3482). https://doi.org/10.3390/molecules29153482

Eweis, A. A., El-Raheem, H. A., Ahmad, M. S., Hozzein, W. N., & Mahmoud, R. (2024). Green Fabrication of Nanomaterials Using Microorganisms as Nano-Factories. *Journal of Cluster Science*, *35*(7), 2149–2176. https://doi.org/10.1007/s10876-024-02660-7

Fitriannisa, I., Draviana, H. T., Hsieh, C. P., Saukani, M., Tzou, K. Y., & Kuo, T. R. (2025). Unveiling the Antibacterial Efficacy and Mechanistic Insights of MnO2 Nanoparticles for Advanced Therapeutic Applications. *International Journal of Molecular Sciences*, *26*(18), 1–16. https://doi.org/10.3390/ijms26189104

Ghosh, S., Nandi, S., & Basu, T. (2022). Nano-Antibacterials Using Medicinal Plant Components: An Overview. *Frontiers in Microbiology*, *12*(February), 1–16. https://doi.org/10.3389/fmicb.2021.768739

Gul, S., Sheoran, S., & Mahlawat, V. (2025). *MnO 2 nanostructures : A review of synthesis methodsand multifunctional*. *12*(2), 1–14. https://doi.org/10.62110/sciencein.mns.2025.v12.1197

Hano, C., & Abbasi, B. H. (2022). *Plant-Based Green Synthesis of Nanoparticles : Production, Characterization, and Applications*. 1–9.

Hessien, M. A., Khattab, R. M., & Sadek, H. E. H. (2025). Synthesis and Characterization of ZnO, Mn3O4, and ZnMn2O4 Spinel by New Chelation-Precipitation Method: Magnetic and Antimicrobial Properties. *Journal of Inorganic and Organometallic Polymers and Materials*, *35*(5), 3739–3758. https://doi.org/10.1007/s10904-024-03489-3

Horti, N. C., Samage, A., Halakarni, M. A., Chavan, S. K., Inamdar, S. R., Kamatagi, M. D., & Nataraj, S. K. (2024). Optical and electrochemical properties of manganese oxide (Mn3O4) nanoparticles: Investigating the influence of calcination temperature on supercapacitor performance. *Materials Chemistry and Physics*, *318*, 129276. https://doi.org/https://doi.org/10.1016/j.matchemphys.2024.129276

Hung, S. C., Chou, Y. R., Dong, C. Di, Yang, W. D., & Tsai, K. C. (2020). Enhanced activity of

hierarchical nanostructural birnessite-MnO2-based materials deposited onto nickel foam for efficient supercapacitor electrodes. *Nanomaterials*, *10*(10), 1–16. https://doi.org/10.3390/nano10101933

Ishfaq, A., Shahid, M., Nawaz, M., Ibrar, D., Hussain, S., Shahzad, T., Mahmood, F., Rais, A., Gul, S., Gaafar, A. R. Z., Hodhod, M. S., & Khan, S. (2023). Remediation of wastewater by biosynthesized manganese oxide nanoparticles and its effects on the development of wheat seedlings. *Frontiers in Plant Science*, *14*(December). https://doi.org/10.3389/fpls.2023.1263813

Jiang, Y., Xiao, M., Lu, Y., Chang, H., & Meng, Y. (2025). Preparation and modification of manganese dioxide and its research progress in energy storage and conversion applications. *SustainableMaterialsandTechnologies*,*46*,e01761.https://doi.org/https://doi.org/10.1016/j.susmat.2025.e01761

Jiang, Y., Zhao, J., & Zhang, D. (2024). Manganese Dioxide-Based Nanomaterials for Medical Applications. *ACS Biomaterials Science & Engineering*, *10*(5), 2680–2702. https://doi.org/10.1021/acsbiomaterials.3c01852

K.K., A. V., & Gangadharan, D. (2022). Adsorptive remediation of organic pollutants and arsenic (V) ions from water using Fe3O4-MnO2 nanocomposite. *Nano-Structures & Nano-Objects*, *29*, 100837. https://doi.org/https://doi.org/10.1016/j.nanoso.2022.100837

Kang, S., Wang, C., Chen, J., Meng, T., & E J. (2023). Progress on solvo/hydrothermal synthesis and optimization of the cathode materials of lithium-ion battery. *Journal of Energy Storage*, *67*, 107515. https://doi.org/https://doi.org/10.1016/j.est.2023.107515

Karthik, P., Jose, P. A., Chellakannu, A., Gurusamy, S., Ananthappan, P., Karuppathevan, R., Vasantha, V. S., Rajesh, J., Ravichandran, S., & Sankarganesh, M. (2024). Green synthesis of MnO2 nanoparticles from Psidium guajava leaf extract: Morphological characterization, photocatalytic, and DNA/BSA interaction studies. *International Journal of Biological Macromolecules*,*258*,128869. https://doi.org/https://doi.org/10.1016/j.ijbiomac.2023.128869

Karthik, P., Mirunya, B., Ayyalsamy, B., Shanmugapriya, S. P., & Rajesh, J. (2025). Eco-friendly synthesis of manganese dioxide nanoparticles using Phyllanthus acidus leaf: Assessing their potential photocatalytic activity against organic dyes. *Surfaces and Interfaces*, *74*, 107716. https://doi.org/https://doi.org/10.1016/j.surfin.2025.107716

Li, H., Fu, B., Huang, H., Wu, S., Ge, J., Zhang, J., Li, F., & Qu, P. (2022). Catalytic degradation

of organic pollutants by manganese oxides: a comprehensive review. *Environmental Pollutants and Bioavailability*, *34*(1), 395–406. https://doi.org/10.1080/26395940.2022.2123047

Li, Z., Sun, Y., Ge, S., Zhu, F., Yin, F., Gu, L., Yang, F., Hu, P., Chen, G., Wang, K., & Volinsky, A. A. (2023). *An Overview of Synthesis and Structural Regulation of Magnetic Nanomaterials Prepared by Chemical Coprecipitation*.

Lu, M., Ma, Y., Li, D., Jiang, M., & Yu, C. (2023). Hydrothermal Synthesis of MnO2 Microspheres and Their Degradation of Toluene. *ACS Omega*, *8*(51), 49150–49157. https://doi.org/10.1021/acsomega.3c07306

Lung, I., & Stegarescu, A. (2023). *Biosynthesis of Nanoparticles Using Plant Extracts and Essential Oils*.

Malhotra, M., Poonia, K., Singh, P., Khan, A. A. P., Thakur, P., Van Le, Q., Helmy, E. T., Ahamad, T., Nguyen, V.-H., Thakur, S., & Raizada, P. (2024). An overview of improving photocatalytic activity of MnO2 via the Z-scheme approach for environmental and energy applications. *Journal of the Taiwan Institute of Chemical Engineers*, *158*, 104945. https://doi.org/https://doi.org/10.1016/j.jtice.2023.104945

Malik, A. Q., Mir, T. ul G., Kumar, D., Mir, I. A., Rashid, A., Ayoub, M., & Shukla, S. (2023). A review on the green synthesis of nanoparticles, their biological applications, and photocatalytic efficiency against environmental toxins. *Environmental Science and Pollution Research*, *30*(27), 69796–69823. https://doi.org/10.1007/s11356-023-27437-9

Martínez-cabanas, M., López-garcía, M., Rodríguez-barro, P., Vilariño, T., Lodeiro, P., Herrero, R., Barriada, J. L., & de Vicente, M. E. S. (2021). Antioxidant capacity assessment of plant extracts for green synthesis of nanoparticles. *Nanomaterials*, *11*(7), 1–14. https://doi.org/10.3390/nano11071679

Matsui, T., Watanabe, H., Somekawa, S., Yanagida, S., Oaki, Y., & Imai, H. (2024). The size-dependent valence and conduction band-edge energies of Cu quantum dots. *Chemical Communications*, *60*(33), 4419–4422. https://doi.org/10.1039/d4cc00260a

Mohite, D. D., Chavan, S. S., Lokhande, P. E., Karandikar, P. B., Londhe, P. V, Rednam, U., Ahsan, W., & Mohite, V. B. (2025). Effect of ball milling jar geometry on MnO2 nanoparticle morphology and supercapacitor performance. *Chemistry of Inorganic Materials*, *7*, 100117. https://doi.org/https://doi.org/10.1016/j.cinorg.2025.100117

Mokaba, P. L., Gazu, N. T., Makinita, M. L., Mthombeni, N. H., Ntola, P., & Feleni, U. (2024). Manganese Oxide Applications in Sulfonamides Electrochemical, Thermal, and Optical Sensors: A Short Review. *Electrocatalysis*, *15*(6), 421–437. https://doi.org/10.1007/s12678-024-00890-x

Muthukrishnan, S., Bhakya, S., & Ramalingam, V. (2025). Metal nanoparticles synthesis: an overview of different synthesis methods, mode of action, and their biomedical application. *Discover Applied Sciences*, *7*(10), 1079. https://doi.org/10.1007/s42452-025-07210-y

Nguyen, N. T. H., Tran, G. T., Nguyen, N. T. T., Nguyen, T. T. T., Nguyen, D. T. C., & Tran, T. Van. (2023). A critical review of the biosynthesis, properties, applications, and future outlook of green MnO2 nanoparticles. *Environmental Research*, *231*, 116262. https://doi.org/https://doi.org/10.1016/j.envres.2023.116262

Ogunyemi, S. O., Zhang, M., Abdallah, Y., Ahmed, T., Qiu, W., Ali, M. A., Yan, C., Yang, Y., Chen, J., & Li, B. (2020). The Bio-Synthesis of Three Metal Oxide Nanoparticles (ZnO, MnO2, and MgO) and Their Antibacterial Activity Against the Bacterial Leaf Blight Pathogen. *Frontiers in Microbiology*, *11*(December), 1–14. https://doi.org/10.3389/fmicb.2020.588326

Oliveira da Silva, J. D., dos Santos, H. C., Bento, G. S., Oliveira, J. F. R., de Souza Abud, A. K., & Gimenez, I. de F. (2024). Green synthesis of manganese dioxide (MnO2) nanoparticles produced with acerola (Malpighia emarginata) leaf extract. *Materials Chemistry and Physics*, *315*, 128963. https://doi.org/https://doi.org/10.1016/j.matchemphys.2024.128963

Plakia, L., & Kartsonakis, I. A. (2025). A Review on Design, Synthesis, and Application of Composite Materials Based on MnO2 for Energy Storage. *Energies*, *18*(13). https://doi.org/10.3390/en18133455

Pole, R. P. P., Doss, A., David, S. A., Kabir, N. A., & Satheesh, S. (2025). Green synthesis of MnO2 nanoparticles using Justicia adhatoda leaf extract. *Sustainable Chemistry One World*, *7*, 100072. https://doi.org/https://doi.org/10.1016/j.scowo.2025.100072

Radulescu, D.-M., Surdu, V.-A., Ficai, A., Ficai, D., Grumezescu, A.-M., & Andronescu, E. (2023). Green Synthesis of Metal and Metal Oxide Nanoparticles: A Review of the Principles and Biomedical Applications. In *International Journal of Molecular Sciences* (Vol. 24, Issue 20, p. 15397). https://doi.org/10.3390/ijms242015397

Salvador, G. M. S., Silva, A. L., Silva, L. P. C., Passos, F. B., & Carvalho, N. M. F. (2021).

Enhanced activity of Pd/α-MnO2 for electrocatalytic oxygen evolution reaction. *International Journal of Hydrogen Energy*, *46*(53), 26976–26988. https://doi.org/https://doi.org/10.1016/j.ijhydene.2021.05.168

Saod, W. M., Hamid, L. L., Alaallah, N. J., & Ramizy, A. (2022). Biosynthesis and antibacterial activity of manganese oxide nanoparticles prepared by green tea extract. *Biotechnology Reports*, *34*, e00729. https://doi.org/https://doi.org/10.1016/j.btre.2022.e00729

Shanshool, S. K., Shanan, Z. J., & Shanan, Z. J. (2024). *Green Synthesis of Manganese Dioxide Nanoparticles and its Biological Green Synthesis of Manganese Dioxide Nanoparticles and its Biological Applications*. *21*(5).

Suryawanshi, P. S., Patil, A. V, Padhye, G. G., Tupe, U. J., Village, T., & Pratishthan, V. D. (2023). *A Review : Synthesis, characterizations, applications, and future perspectives of Manganese dioxide nanoparticles and nanostructures*. *71*(10), 196–215.

Tadesse, S. H., & Hailemariam, T. T. (2025). *A Review on the Classification, Characterisation, Synthesis of Nanoparticles and Their Application*. *6*(2), 63–72.

Thatyana, M., Dube, N. P., Kemboi, D., Manicum, A. E., Mokgalaka-fleischmann, N. S., & Tembu, J. V. (2023). *Advances in Phytonanotechnology : A Plant-Mediated Green Synthesis of Metal Nanoparticles Using Phyllanthus Plant Extracts and Their Antimicrobial and Anticancer Applications*.

Ula, F., Yüksel, E., Dinçer, D., & Dababat, A. (2025). *Recent Advances in Plant-Based Green Synthesis of Nanoparticles : A Sustainable Approach for Combating Plant-Parasitic Nematodes*. 1–12.

Vanga, S., & Satla, S. R. (2025). A review on green synthesis, characterization, and applications of plant-mediated metal nanoparticles. *Next Research*, *2*(2), 100356. https://doi.org/https://doi.org/10.1016/j.nexres.2025.100356

Velho Pereira, S., Naik, S. R., Naik, A., Shekupa, R., Palkar, V., Shaikh, F., & Naik-Samant, S. (2026). Exploring the multifaceted applications of manganese dioxide nanoparticles: Antibacterial, antibiofilm, antioxidant, and hemolytic activities. *Materials Chemistry and Physics*, *347*, 131474. https://doi.org/https://doi.org/10.1016/j.matchemphys.2025.131474

Yadav, P., & Bhaduri, A. (2023). Chemically synthesized manganese oxide nanorods for effective organic dye removal and energy storage applications. *Materials Chemistry and Physics*, *299*, 127495. https://doi.org/https://doi.org/10.1016/j.matchemphys.2023.127495

Yang, P., Wang, J., Wang, H., Wang, S., Yang, C., & He, Y. (2023). Physicochemical properties of different crystal forms of manganese dioxide prepared by a liquid phase method and their quantitative evaluation in capacitor and battery materials. *Nanoscale Advances*, *5*(12), 3396–3413. https://doi.org/10.1039/d3na00144j

Zhang, X., Sathiyaseelan, A., Naveen, K. V., Lu, Y., & Wang, M.-H. (2023). Research progress in green synthesis of manganese and manganese oxide nanoparticles in biomedical and environmental applications – A review. *Chemosphere*, *337*, 139312. https://doi.org/https://doi.org/10.1016/j.chemosphere.2023.139312

Zhydzetski, A., Głowacka-Grzyb, Z., Chlebicka, K., & Władyka, B. (2025). Detection and identification of pathogens using agents targeting the bacterial cell wall. *Folia Microbiologica*. https://doi.org/10.1007/s12223-025-01379-w